2017

Kentucky Water Resources Research Institute Annual Technical Report FY 2016

Digital Object Identifier: https://doi.org/10.13023/kwrri.katr.2016

Kentucky Water Resources Research Institute, University of Kentucky

Kentucky Water Resources Research Institute
Annual Technical Report
FY 2016

Introduction

The 2016 Annual Technical Report for Kentucky consolidates reporting requirements for the Section 104(b) base grant award into a single document that includes: 1) a synopsis of each student research enhancement project that was conducted during the period, 2) citations for related publications, reports, and presentations, 3) a description of information transfer activities, 4) a summary of student support during the period, and 5) notable awards and achievements.

No funds were requested for general program administration activities. However, travel funds were provided to support the participation of the director and associate director in the annual meeting of the National Institutes for Water Resources in Washington, DC from February 27 - March 1, 2017.

Research Program Introduction

The activities supported by the Section 104(b) program funds and required matching are interwoven into the overall program of the Kentucky Water Resources Research Institute. Additional research, service, and technology transfer activities were funded through a variety of other sponsors. The Kentucky River Authority supported watershed management services in in the Kentucky River basin and a small grant program to fund local grassroots watershed organizations. The National Institute of Environmental Health Services supported research translation activities through the Superfund Public Outreach Program and the development of ground water remediation processes for potential use a contaminated sites. Beam Suntory supported two summer intern students to conduct studies of water availability and use at the Kentucky distilleries.

The Institute's Committee on Research and Policy considered 16 proposals for student research enhancement grants for support through 104(b) 2016 funding. Nine projects were selected. The projects were conducted at the University of Kentucky (7), the University of Louisville (1), and Morehead State University (1). The projects represented faculty and students from a variety of discipline areas including civil engineering (1), chemistry (1), applied geography (1), forestry (1), geosciences (1), biosystems and agricultural engineering (2), biology (1), and plant and soil science (1). The goal of this approach is to support a number of student-based efforts representing a variety of discipline areas at numerous educational institutions throughout the state to support broad research capacity related to water resources. It is critical that students are trained for the workforce in government, private industry, and academia. A total of 13 students participated in 2016 104(b) projects (4 PhD, 4 MS, 5 undergraduate students). Reports for the nine projects follow.

Selenium removal by biological processes in water supplies

Basic Information

Title:	Selenium removal by biological processes in water supplies
Project Number:	2016KY254B
Start Date:	3/1/2016
End Date:	2/28/2018
Funding Source:	104B
Congressional District:	KY 6th
Research Category:	Water Quality
Focus Category:	Hydrogeochemistry, Toxic Substances, Water Quality
Descriptors:	None
Principal Investigators:	Yi-Tin Wang

Publications

1. Ji, Yuxia, and Y.T. Wang, 2017, Selenium Reduction by Batch Cultures of Escherichia coli Strain EWB32213, ASCE Journal of Environmental Engineering,143 (6).
2. Ji, Juxia, and Y.T. Wang, 2016, Selenium Reduction in Batch Reactors, in Proceedings of the Water, Wastewater, Stormwater, and Watershed Symposium of the ASCE EWRI Conference, May 22-26, 2016, West Palm Beach, Florida, p. 175-180.
3. Ji, Yuxia, and Y.T. Wang, 2017 Selenium Reduction by a Co-Culture of Pantoea Vagans Strain EWB32213-2 and Shigella Fergusonii Strain TB42616, in Proceedings of the 2017 Kentucky Annual Water Resources Symposium, Kentucky Water Resources Research Institute, Lexington, KY, p. 35-36.

Selenium Removal by Biological Processes in Water Supplies

Problem and Research Objectives

Selenium occurs naturally and is an essential nutrient in small amounts. It is toxic to aquatic life at very low levels and can also be harmful to human health. Anthropogenic sources of selenium are wide spread including electronic and photography, glass manufacturing, pigments, additives for metal processing, copper refining operations, fossil fuel combustion, petroleum refining, and agricultural drainage waters in the Western United States. In Eastern Kentucky, surface-mining operations in Appalachian coal regions have been identified as the major cause of selenium contamination in water and fish, due to the prevalence of selenium in overburden soils exposed during mining activities.

Exposure to very high levels of selenium can cause dizziness, fatigue, irritation, collection of fluid in the lungs, and severe bronchitis. The U.S.EPA has established a chronic standard for selenium in freshwater at 5 μg/L and a maximum contaminant level for selenium in drinking water at 0.05 mg/L.

Selenium occurs in various forms in the environment. The oxidized forms, selenate (Se (VI)) and selenite (Se (IV)), are soluble and mobile and are found in well aerated conditions. In reducing environments, however, the elemental selenium (Se (0)) which is insoluble in water, and various selenides (-II) are the predominate species. Speciation of selenium depends on environmental factors such as pH, redox potential, complexing ability of ligands, and biological interactions. Selenium reduction has been observed in lake sediments, agricultural drain sediments, wetland sediments and in coal mine tailings pond sediment. A USGS study revealed that Kentucky has the highest average concentration of selenium in coal of any Central Appalachian state at 4.2 ppm, a level likely to result in stream selenium concentrations higher than 5 μg/L.

Selenium in water was usually reduced through contact with a metal reductant under acidic conditions and then removed by the coagulation-sedimentation method. With this conventional approach, however, selenate at high concentration could not be effectively removed and the cost of the chemicals used for the reduction of selenate is high. In addition, a large amount of sludge is generated as a byproduct.

In this study, we evaluate the potential of biological processes as an efficient, cost-effective alternative for selenium reduction in water supplies. Laboratory experiments were conducted to assess the environmental factors affecting selenium reduction with a selenium-reducing strain isolated in our laboratory. Batch cultures were used to determine the effect of environmental factors such as temperature, pH, selenium concentration, and selenium co-contaminants on selenium reduction. Based on the batch results, the appropriate pH, and temperature were selected for study using a bench-scale, continuous-flow bioreactor.

The overall objective of the proposed study is to obtain a better understanding of selenium reduction in aqueous environment by microbial activities. The specific aims were:

1. To determine environment factors affecting microbial reduction of selenium.
2. To evaluate the toxicity of co-contaminants found in coal mining and processing operations on selenium reduction by microbial activities.
3. To develop kinetic expressions and a mathematical model for selenium reduction incorporating the above factors.
4. To evaluate selenium reduction and recovery potential in continuous-flow bioreactor systems.

Methodology

This study was initiated with batch cultures of *E. coli* strain EWB32213. This selenium-reducing strain was isolated in our laboratory from sediments of the slurry pond at the E.W.Brown Generating Station in Harrodsburg, KY. Se(VI)-reducing *Shigella fergusonii* strain TB42616 and Se(IV)-reducing *Pantoea vagans* strain EBW32213-2 were isolated from Town Branch Wastewater Treatment Plant in Lexington, KY, and the slurry pond at E.W. Brown Station, respectively. Batch cultures were used to evaluate the effect of the following variables on relative rates of Se(VI) and Se(IV) reduction: Concentrations of growth substrate, Se(VI) , Se(IV), temperature, and pH. Glucose was used as the growth substrate. Se(VI) and Se(IV) concentrations were evaluated from 10 to 400 mg/L and temperature was investigated from 10^{o}C to 50^{o} C while pH varied from 4 to 9.

Based on the batch results, the appropriate pH, and temperature were selected for study using a bench-scale, continuous-flow bioreactor. The bioreactor consists of jell-bead packed Pyrex glass column operated in upflow mode. Jell beads were used to immobilize Se(VI)- reducing strains in the continuous-flow bioreactor.

The entrapment and encapsulation of the bacterial cells using alginate gel is achieved by the gentle destabilization of high concentrations of non-gel-inducing ions such as Na^{+}. A 4% (w/v) aqueous solution of Na-alginate was prepared by suspending the polymer into the distilled water. The suspension was stirred by a magnetic stirrer and left overnight under room temperature after autoclave at 121℃ for 15 minutes. Sterilized alginate solution was then mixed with an equal volume suspension of the harvested bacterial cells washed by 0.85% (w/v) NaCl. The spherical gel beads were formed by dripping the alginate-cell suspension into an autoclaved 2%(w/v) CaCl solution using a dropper.

Principal Findings and Significance

The effect of pH on selenium reduction by E. coli EWB32213 was investigated at pHs 4, 5, 6, 7, 8, 9, and 10, respectively, at 30℃ in a temperature control room. The results in Figure 1 show that Se(VI)reduction to Se(0) was highest (81.27-84.78%) at pH 6-8 after 5-day incubation with rapid decreases outside this range. Little selenate reduction was observed at pH 4, and the Se(VI) reduction rate (55.93%) was significantly lower at pH 9 than at pH 6-8 (Fig. 1). Similarly, the optimal pH of Se(VI) reduction by *Shigella fergusonii* strain TB42616 was observed at pH 8 and *Pantoea vagans* strain EBW32213-2 reduced Se(IV) best at pH 7.

An optimal temperature of 30-40℃ for Se(VI) reduction to Se(0) by *E. coli* strain EWB32213 was also observed. The data indicate that Se(VI) reduction rate increased with temperature when it was lower than 30℃, stabilized at 30-40℃, and then followed by rapid decrease when temperature was above 40℃. Little Se(VI) reduction was observed above 50℃ or lower than 10℃. The highest Se(VI) reduction observed was nearly 86% at 30‑40℃ after 5-day incubation. Subsequently, selenium reduction experiments with strain EWB 32213 were conducted at pH 7 and 30℃(Fig. 2). Similarly, the optimal temperature of Se reduction by *Shigella fergusonii* strain TB42616 was observed at 40 ℃. The *Pantoea vagans* strain EBW32213-2 optimum was 30 ℃.

No significant effect on the rate of Se reduction by these three strains was noted even at Se concentration as high as 400 mg/L.

Se(VI) reduction is a two-stage process with the second step of Se(IV) reduction to elemental Se, Se(0) being the rate-limiting one. In order to accelerate the overall Se(VI) reduction rate, we are investigating a defined co-culture of Se(VI)-reducing *Shigella fergusonii* strain TB42616 and Se(IV)-reducing *Pantoea vagans* strain EBW32213-2 in batch reactors. Preliminary results indicate that the rate of Se(VI) reduction is faster in the co-culture as compared to pure culture of TB42616 as displayed by the intensity of red color from reduced Se (0) (Fig. 3). Presently, we are looking into factors such as electron donors, and ratio of the two cultures in order to find the optimal conditions of Se(VI) reduction.

Simultaneously, we are investigating Se(VI) reduction in continuous-flow bioreactor. However, we have found that Se (VI) reduction in continuous-flow bioreactor is not feasible unless a sufficient amount of cells can be maintained in the reactor to overcome the slow growth rate and loss rate. Currently, we are investigating a bioreactor packed with gel beads containing Se-reducing species (Fig. 4). The reactor column is 12 cm long, with an inner diameter of 2.3 cm and is packed with 1661 gel beads of 0.3 cm average diameter. The liquid detention time will be in the range of a few days to a few hours. After steady-state conditions are reached, the fate of Se in the bioreactor will be analyzed by material balance. We will develop a sophisticated mathematic model incorporating mass balance, molecular diffusion, reaction kinetics, and reactor flow characteristics. We will also investigate Se reduction efficiency of the continuous-flow reactor using gel-bead-immobilized-defined co-culture depending upon what is found from our batch studies during the 2017-2018 no-cost extension period.

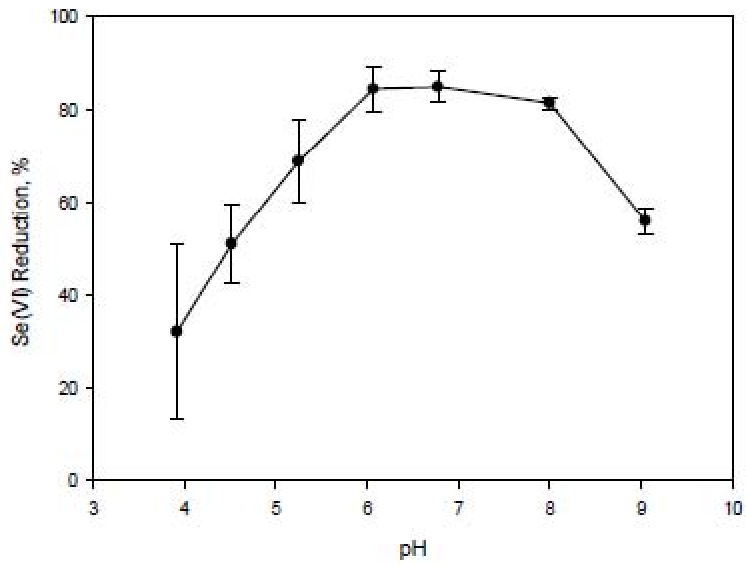

Figure 1. Effect of pH on selenium reduction after 5 days.

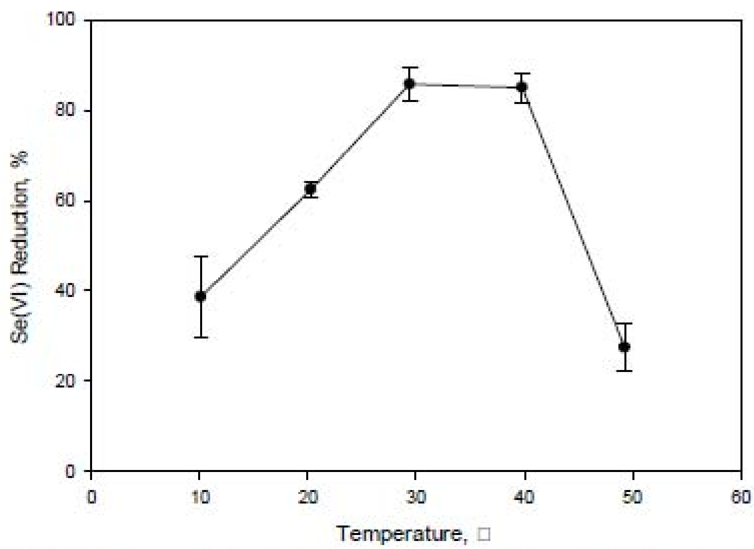

Figure 2. Effect of temperature on selenium reduction after 5 days.

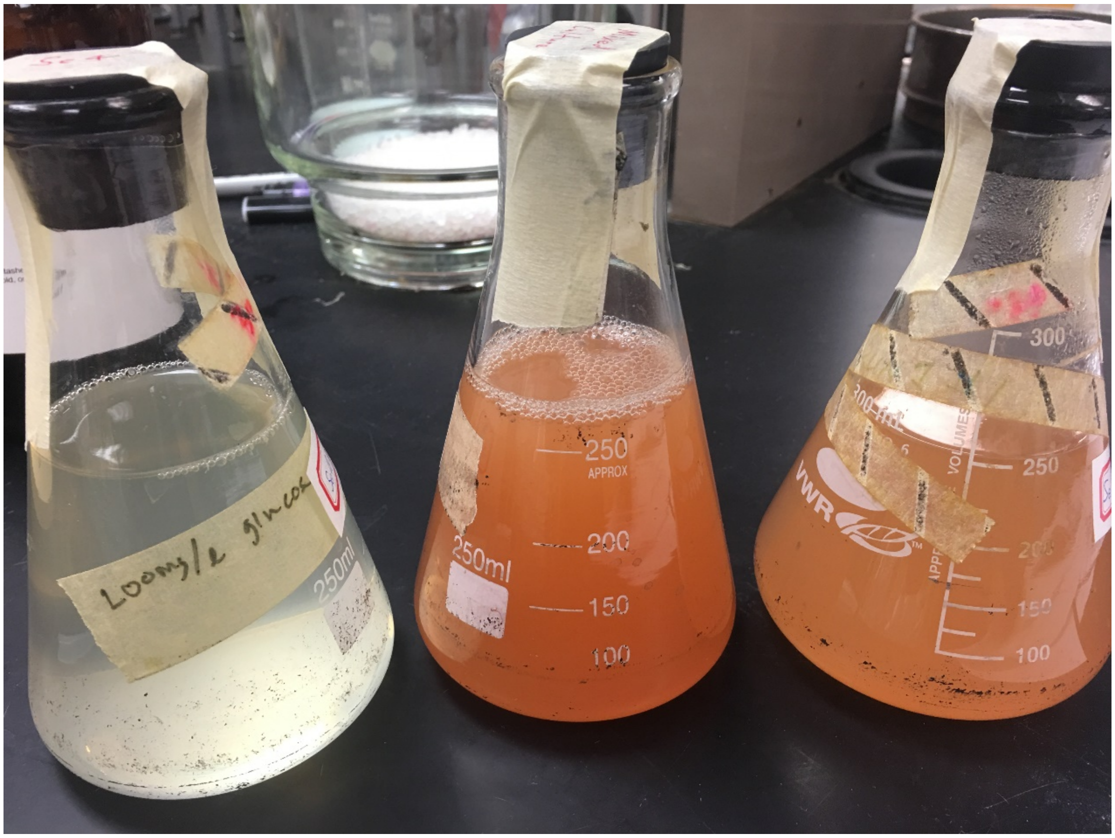

Figure 3. Preliminary study of Se Reduction by (a) pure culture of TB42616-left flask, (b) defined co-culture of TB42616 and EWB32213-2-center flask, and (c) pure culture of EWB32213-2-right flask.

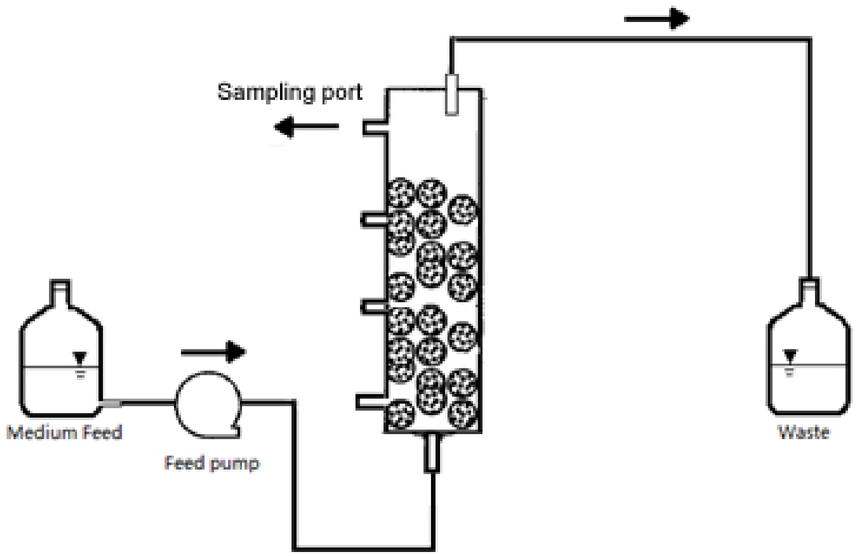

Figure 4. Schematic diagram of the packed-bed reactor system

Novel methods for the incorporation of AqpZ water channel protein in membranes for water filtration

Basic Information

Title:	Novel methods for the incorporation of AqpZ water channel protein in membranes for water filtration
Project Number:	2016KY255B
Start Date:	3/1/2016
End Date:	2/28/2017
Funding Source:	104B
Congressional District:	KY 6th
Research Category:	Water Quality
Focus Category:	Treatment, Water Quality, Water Use
Descriptors:	None
Principal Investigators:	Yinan Wei

Publication

1. Abeywansha, Thilini, Xinyi Zhang, and Yinan We, 2017, Effect of Histag on the Production of Water Channel Protein AqpZ, in Proceedings of the 2017 Kentucky Water Resources Annual Symposium, Kentucky Water Resources Research Institute, Lexington, KY, p. 97.

Novel Methods for the Incorporation of AqpZ Water Channel Protein

Project and Research Objectives

Aquaporin Z (AqpZ) is the water channel from bacterium *Escherichia coli* (*E. coli*) (Figure 1). It is the protein of choice for many research groups worldwide in their work to incorporate water channel proteins into selective membranes for water filtration. In most of these studies, AqpZ extracted from *E. coli* membrane are directly embedded into a polymer matrix. No attempt has been reported to covalently attach AqpZ into the matrix or to control the direction of its immobilization. In this study, we developed molecular engineering strategies to covalently and directionally immobilize AqpZ. The two research objectives were to : 1) install functional groups on AqpZ for covalent attachment into a polymer matrix; and 2) generically engineer functional AqpZ constructs to enable directional immobilization.

Methods and Procedures

In this research project, the graduate student research assistant (Thilini Abeywansha) worked on the development of approaches identified in the original proposal and completed her work on both proposed objectives. For objective one, she experimented with the metabolic incorporation of an unnatural amino acid azidohomoalanine (AHA) into the sequence of AqpZ. For objective two, she investigated three proposed methods. AqpZ with the proposed modifications was constructed and its interaction with the corresponding surface was studied. Specifically, AqpZ bearing a histag at the C-terminus was created and its binding to a metal affinity surface studied. A unique reactive sulfhydryl functional group was introduced at the N-terminus of AqpZ, and interaction with maleimide or free sulfhydryl surface was tested. Finally, an avitag was introduced at the C-terminal of AqpZ and it was demonstrated that the tag can facilitate in vivo biotinylation, which enables subsequent binding to an avidin surface.

Principal Findings and Significance

To obtain AqpZ for study, we cloned the gene of AqpZ into an expression vector, overexpressed the protein in *E. coli*, and finally extracted and purified the protein. Histag, which is a short peptide of six histidine residues, is a popular tag for protein purification and immobilization. At the beginning of this project, we first experimented with the location of histag and studied its effect on AqpZ expression. Five different AqpZ histag constructs were created. The first four contained histag at the C-terminus of the protein, with linkers of different lengths (Figure 1). Since AqpZ is a membrane protein and needs to be co-translationally inserted into the cytoplasmic membrane, we first decided to try constructs with histag at the C-terminus to avoid potential effect on the interruption of membrane insertion, since the first transmembrane helix at the N-terminus is considered the signal for membrane integration.

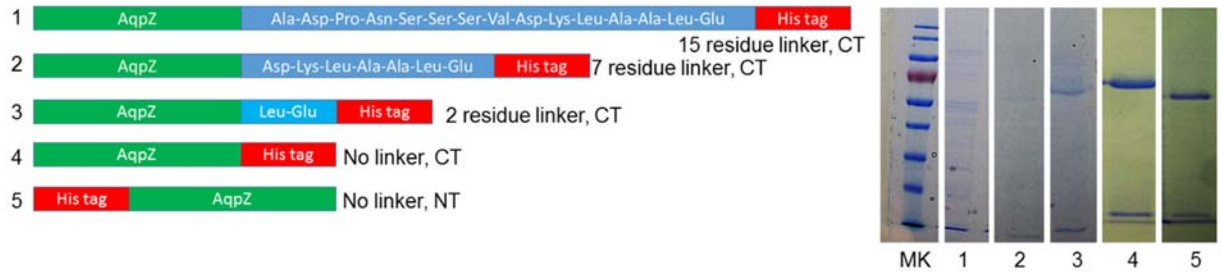

Figure 1. AqpZ constructs created in this study, with C-terminal histag (1-4, CT) or N-terminal histag (5, NT) and their expression levels. Lane MK is the protein molecular weight marker. From top to bottom, the molecular weights of the bands are 180, 130, 95, 72 (red), 55, 43, 34, 26, and 17 kD, respectively. The expression level of 15 residue linker-CT histag is similar as the NT-histag construct. While with shorter linkers (7 residues, 2 residues, or no linker), the expression level decreases systematically with the linker length.

The expression and purification of all five constructs were tested. All proteins were expressed in *E. coli* strain BL21(DE3). Proteins were purified from cell lysate with metal affinity chromatography, using Ni-NTA resin. The data showed that the histag could not be introduced directly at the C-terminus of the protein, which greatly reduced the expression of the protein. When the C-terminal histag was used, a spacer sequence of approximately 15 amino acids needs to be included (Figure 1). In contrast, when introduced at the NT, no linker is necessary. For the rest of the study AqpZ with NT histag was used as the base for the introduction of addition modification.

Using this construct, the effect of the incorporation of AHA was tested. When expressed in the Met auxotrophic strain in the presence of AHA, AqpZ cannot be expressed in a significant level. This lack of expression indicates that the replacement of Met using AHA significantly affected the structure/stability of AqpZ. Therefore, the proposed method in Objective 1 did not work. In a separate study, we tested the same protocol using two soluble proteins, green fluorescent protein (GFP) and the enzyme inorganic pyrophosphotase (PpaC). Both proteins can be expressed and retain their activity. The difference in expression behavior might reflect the difference of protein location. It is possible that the AHA incorporation method might work for soluble proteins but not integral membrane proteins. This remains to be tested further.

We introduced a Cys at the N-terminus of AqpZ, which is accessible to reaction or modification via sulfhydryl-specific chemistry. The introduction of Cys right after Met1 at the N-terminus did not affect the expression or purification of AqpZ. The Cys-AqpZ construct will be used in future thiol-specific attachment experiments to examine its performance.

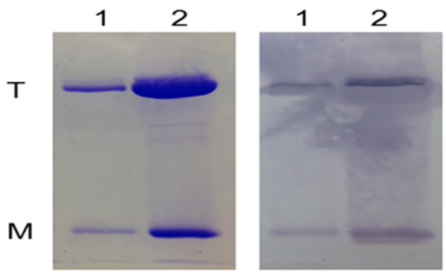

Figure 2. Purification and biotinylation of AqpZ-avitag. Left panel shows the commassie blue stain of two elution fractions indicating the purity of AqpZ sample, right panel are the anti-biotin Western blot of the same two samples, indicating that the proteins are biotinylated. The two bands are monomer (M) and tetramer (T) of AqpZ.

Finally, we introduced an avitag at the C-terminus of AqpZ. The avitag is a peptide of 15 residues that correspond to the biotin ligase BirA recognition site. When expressed in *E. coli* cells, a Lys in the middle of the avitag is biotinylated automatically by BirA in the cytosol of *E. coli*. The purified protein bearing a biotin at the CT, is suitable to subsequent labeling and immobilization studies. Using this strategy, we have successfully generated biotinylated AqpZ. The introduction of the tag does not affect the expression and purification of AqpZ (Figure 2). We have also demonstrated that the purified protein is biotinylated and can be immobilized onto avidin beads, through biotin-avidin interaction. We expect this strategy to be useful in the production of naturally biotinylated function proteins, which can be used in immobilization experiments without further modification.

Assessing the curve number method for modeling urban watersehd stormwater runoff across Louisville, Kentucky

Basic Information

Title:	Assessing the curve number method for modeling urban watersehd stormwater runoff across Louisville, Kentucky
Project Number:	2016KY256B
Start Date:	3/1/2016
End Date:	2/28/2017
Funding Source:	104B
Congressional District:	KY 3rd
Research Category:	Climate and Hydrologic Processes
Focus Category:	Hydrology, Surface Water, Methods
Descriptors:	None
Principal Investigators:	Christopher Andrew Day

Publication

1. Day, C. Andrew and Garrett Seay, 2017, Assessing the Curve Number Method for Modeling Urban Watershed Stormwater Runoff across Louisville, Kentucky, in Proceedings of the 2017 Kentucky Water Resources Annual Symposium, Kentucky Water Resources Research Institute, Lexington, KY, p. 55.

Assessing the Curve Number Method for Modeling Urban Watershed Stormwater Runoff Across Louisville, Kentucky

Problem and Research Objectives

According to the US EPA, when a watershed reaches 75% impervious land cover surface runoff accounts for 55% of precipitation input losses compared to 10% for a 'natural cover' watershed (US EPA, 2003). Consequently, the city of Louisville, KY often experiences localized flooding when frontal systems move in from the northwest to develop severe thunderstorm activity. Based on the National Weather Service Precipitation Frequency Data Server, a typical 2 hour storm event will deposit 1.38-4.51 inches rainfall ranging from a 1-500 year storm recurrence interval (NOAA 2015). A common technique in modeling surface runoff response to storms includes the curve number (CN) method, first developed by the Soil Conservation Service (SCS) in the 1950's. This approach calculates the watershed runoff depth resulting from a storm, with infiltration losses determined by soil and land cover conditions. The CN value applied in the runoff equation reflects these conditions, and is typically chosen from a table of pre-determined values thus defining this method as empirical (USDA 1986). However, subsequent research has identified that the CN chosen for a given soil/land cover condition can be highly sensitive, especially concerning the initial abstraction or losses in stormwater when applying high and low CN values (Hawkins et al. 2005). Consequently additional research discovered that the CN method performed poorly when compared to other physically based stormwater loss methods, such as Green-Ampt, particularly for smaller storm events (Van Mullem 1991).

The objective of this project was to model historical rainfall-runoff processes for 6 small urban watersheds within the city of Louisville for a series of observed storm events in order to assess and calibrate the current empirical CN loss method in comparison to the more physically based Green and Ampt loss method. This approach has been suggested as an alternative method towards improving existing CN values currently employed in urban stormwater studies (Hawkins et al. 2005). The analysis employed emphasizes the importance of carefully selecting and fully testing key parameters in hydrological modeling.

Methodology

The study includes 6 small watersheds across Louisville, first identified in a study by Evaldi and Moore (1994) (Figure 1 and Table 1). Geospatial data sources included:

- -Digital Elevation Model (DEM) data for delineating watersheds (3m resolution, USGS 2016a)
- -Digital orthoimagary for classifying land cover within each watershed (1m resolution, USGS 2016b)
- -Soil hydrologic group and soil class data to determine precipitation losses for the CN and Green and Ampt loss methods (10m resolution, NRCS 2016)

Each watershed was visited in order to record the precise coordinates of their respective outlets. These coordinates were then entered into ArcGIS, and using the DEMs and the hydrology toolset, the watershed boundaries and areas were defined. Following this the mean slope and hydraulic lengths were calculated from the DEMs, both of which were required for the storm runoff modeling component. Next the orthoimagery data allowed a classification of each watershed landcover into 4 groups using a supervised classification technique in ArcGIS (Figure 1). Finally the soil data were overlaid with the landcover classification and, using the 'reclass' tool the landcover and soil layers were combined and assigned initial curve numbers according to the USDA (1986). For the Green and Ampt loss method, the soil class data allowed the 4 key infiltration parameters to be determined: initial moisture content, saturated content, soil suction and hydraulic conductivity (Rawls, Brakensiek and Miller 1983). *This approach differed from the original project proposal which intended using the pre-determined landcover classifications from Evaldi and Moore (1994). However it was decided that a new classification was required in order to account for any possible landcover changes that might have occurred in the intervening years across any of the watersheds.*

Non-geospatial data sources included:

-5 minute precipitation data (point format, MSD 2016)
-5 minute runoff data (obtained using Hobo water level loggers)

Observed precipitation data for 2 storms were obtained for each watershed (excluding SR 4 in which data from a single storm was collected due to time constraints) from the MSD rain gage network (MSD 2017). This network operates a series of telemetered tipping bucket systems which record total rainfall and rainfall intensity for storms at 5 minute intervals. The corresponding discharge data for each storm was recorded using Hobo water level loggers placed in stilling-wells at the stormwater outlet of each watershed. The cross-sectional measurements of each outlet were also recorded so that the water height measurements could be converted to discharges using the manning velocity formula (Dunne and Leopold 1978). *This approach differed from the original project proposal which intended using the storm precipitation and runoff data recorded from Evaldi and Moore (1994). However subsequent research determined that these data were no longer available, requiring a new storm and runoff dataset.*

The geospatial and non-geospatial outputs were applied to the HEC-HMS rainfall-runoff model, first developed by the US Army Corps of Engineers as a lumped-parameter model that routes surface flow towards a basin outlet. One of the benefits of this model is that it allows the user to select various surface infiltration loss methods (e.g. SCS CN, Green and Ampt) when modeling and calibrating surface runoff in response to an observed storm event. This research performed a sensitivity and calibration analysis of the empirical SCS CN loss method compared to the physical Green-Ampt method for each watershed to determine if current CN values accurately reproduce the stormwater runoff volume generated by each storm and which CN values would be most suitable for the Louisville area following any necessary calibration.

Model calibration was achieved by matching the modeled time to peak discharge, size of peak discharge and total runoff volume generated with the observed values (Hejazi and Markus 2009).

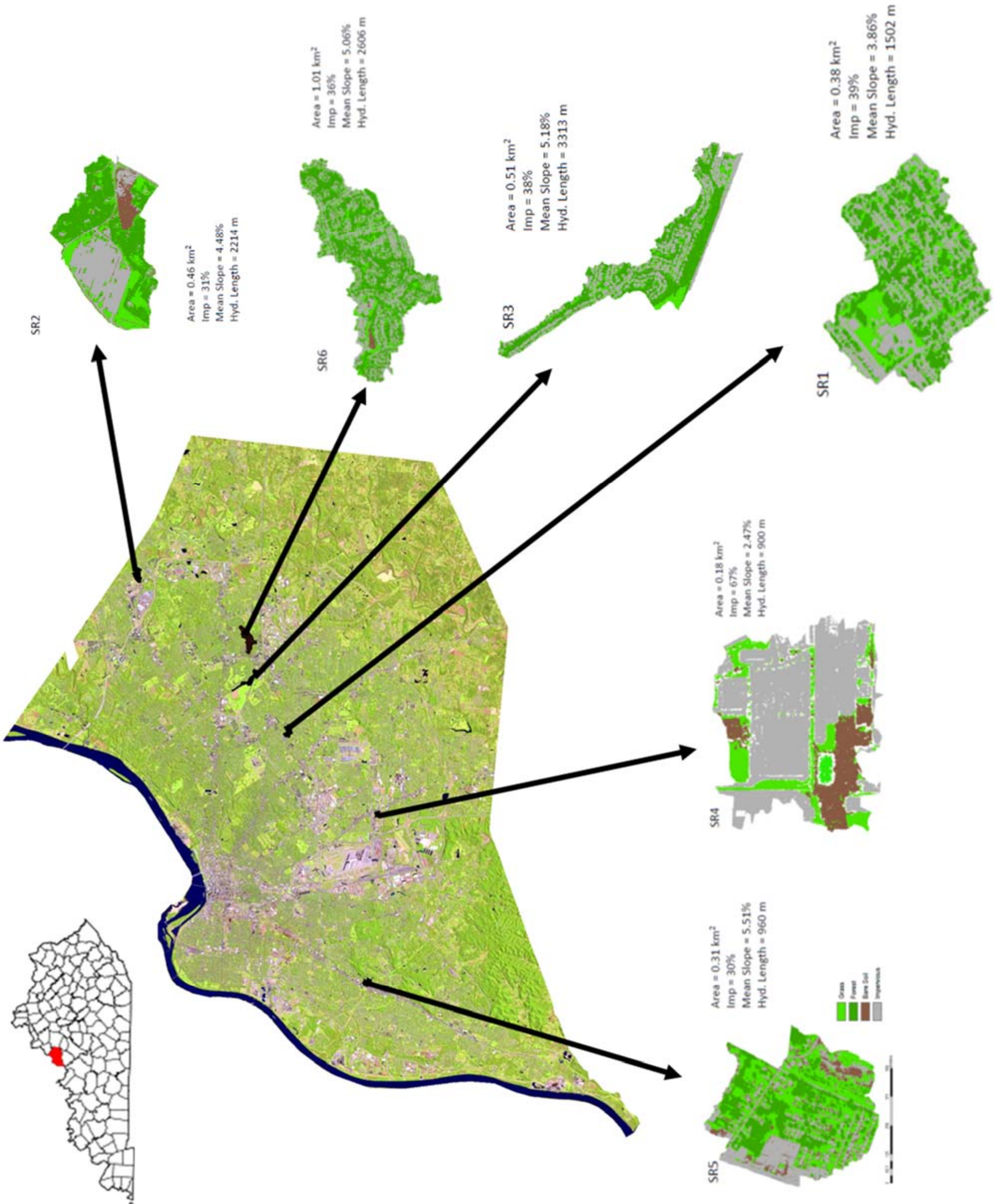

Figure 1. Watersheds included in study, showing location within Jefferson County, classified land covers and key watershed surface variables.

Principal Findings and Significance

Table 1 displays the key physical surface variables of each watershed used to drive the HEC-HMS model.

Watershed	***Area (sq. km)***	***Impervious Cover (%)***	***Slope (%)***	***Hyd. Length (m)***
SR1	0.38	39	3.86	1502
SR2	0.46	31	4.48	2214
SR3	0.51	38	5.18	3313
SR4	0.18	67	2.47	900
SR5	0.31	30	5.51	960
SR6	1.01	36	5.06	2606

Table 1. Key watershed physical surface variables.

Figures 2-7 display the observed storm hyetographs and runoff hydrographs for each storm event per watershed.

Table 2 displays the initial and calibrated CN values and corresponding lag times for each storm per watershed using the CN loss method. With the exception of SR1 and SR5, the model significantly underestimated the stormwater runoff for each storm event. It is noted that these two basins are smaller in area giving shorter hydraulic lengths. Incidentally, while it is recognized that SR4 has the smallest area of all the study watersheds, it also has the greatest impervious cover to potentially negate this effect (see further explanation below). Of further note SR3 required the greatest calibration when running the CN loss method. This is likely due to the fact that his watershed has a much greater hydraulic length compared to the other watersheds. As can be seen in figure 1, this watershed also has a unique shape with the water being funneled down a narrow path towards the storm water outlet which may have significantly contributed to the greater underestimation of stormwater runoff generated by both storms.

When calibrating the runoff models, the CN values most sensitive to change appeared to be those representing grass and forested locations, with the original values being markedly conservative. Of note, SR1 and SR4 required the least CN calibration with both of these watersheds containing the largest overall proportional areas of impervious cover. Despite this, good agreement was generally achieved between the observed and computed runoff for all events following CN calibration (Table 3). For both storms, all mean goodness-of-fit statistics fell below 7% error.

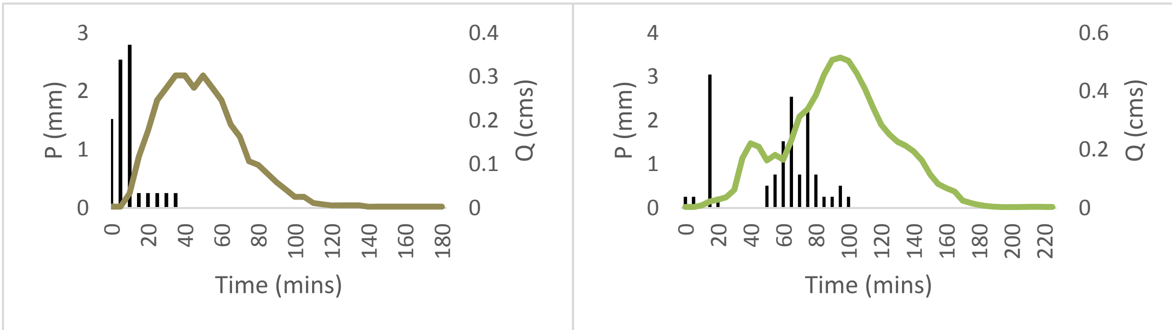

Figure 2. SR1 storm hydrographs.

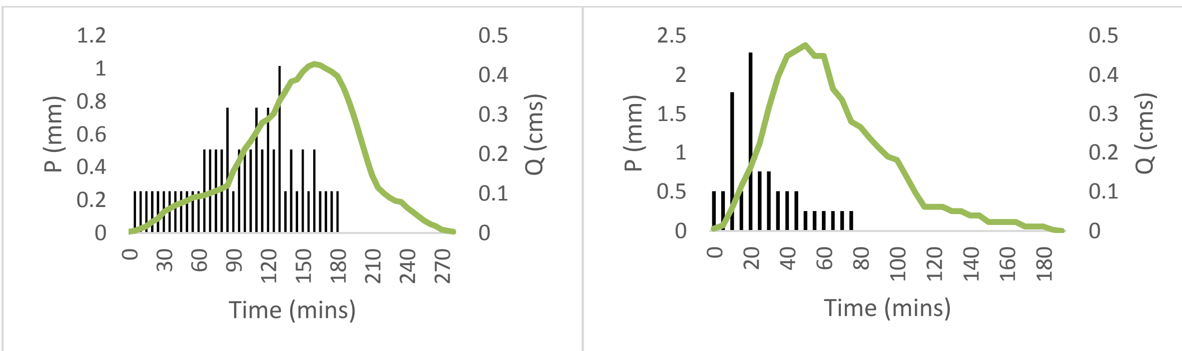

Figure 3. SR2 storm hydrographs.

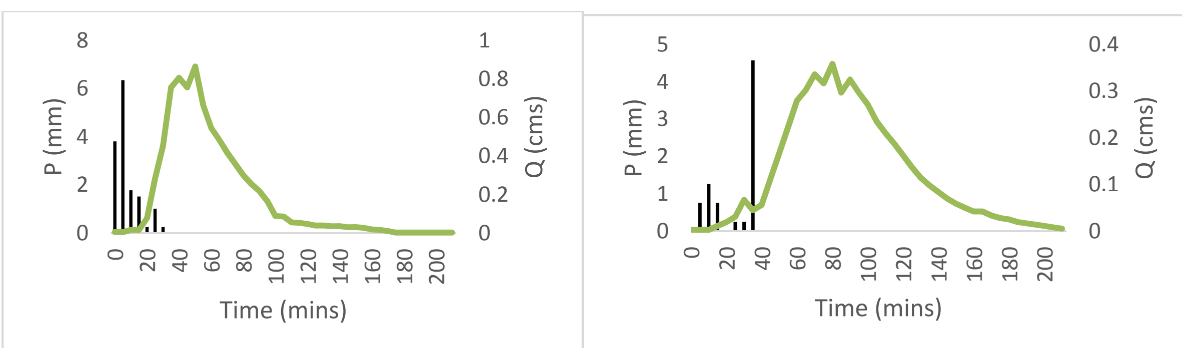

Figure 4. SR3 storm hydrographs.

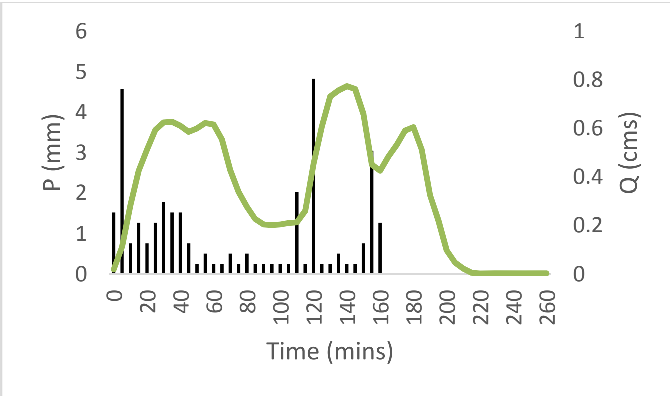

Figure 5. SR4 storm hydrograph.

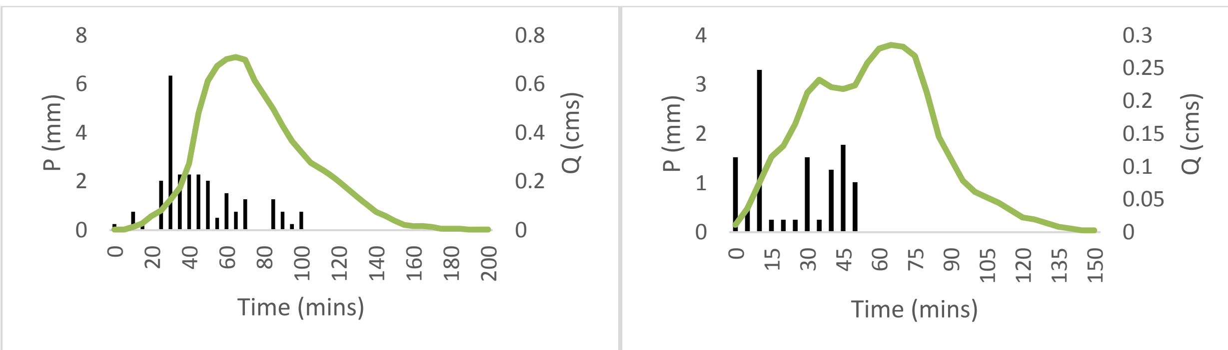

Figure 6. SR5 storm hydrographs.

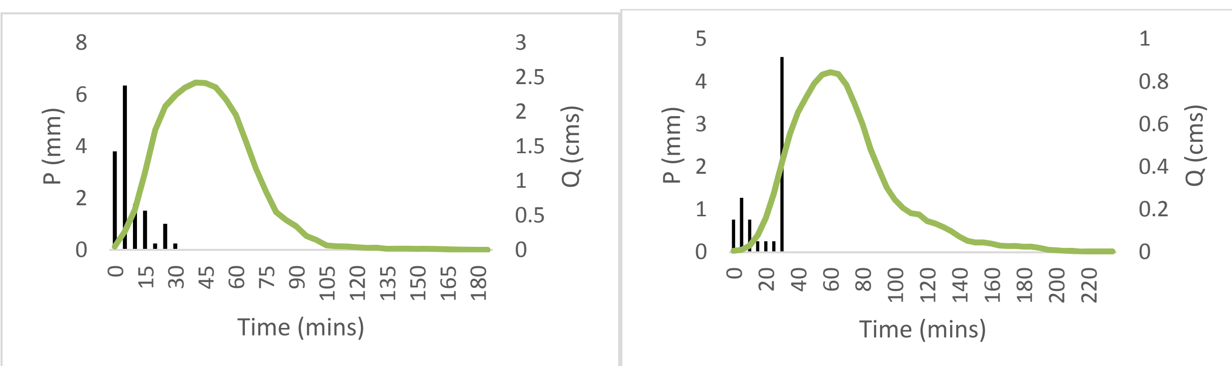

Figure 7. SR6 storm hydrographs.

The largest errors, particularly in the peak and time to peaks occurred for storm 1 for watersheds SR1 and SR3. Interestingly both of these events were strongly left-skewed 'short-burst' storms in that they began very intensely before quickly petering out (Figures 2 and 4), suggesting that the CN loss method struggles to model these precise input conditions. Similarly, larger errors in stormwater runoff volume were noted for SR6 for both storms. These two storms display an extreme left and right skew accordingly suggesting that the CN method struggles to match these particular input conditions when modeling the stormwater volume generated.

Watershed	***Pre Values***		***Storm 1***		***Storm 2***	
	CN	***Lag***	***CN***	***Lag***	***CN***	***Lag***
SR1	85.3	29.2	82.1	32.5	84.2	30.3
SR2	81.4	42.1	91.4	29.1	93	27.1
SR3	75.4	64.8	92.4	35.8	84	49.6
SR4	90.6	19.8	93.5	17.4	-	-
SR5	85.1	17.2	79	21	75.9	23
SR6	83.1	42.6	91.3	31.4	88.8	34.7

Table 2. Pre and calibrated CN and lag times (mins) per storm event.

Watershed	***Storm 1***			***Storm 2***		
	Diff in Peak (%)	***Diff in time to peak (%)***	***Diff in volume (%)***	***Diff in Peak (%)***	***Diff in time to peak (%)***	***Diff in volume (%)***
SR1	5.6	-14.3	-3.3	-1.1	-5	-3.5
SR2	0	-3.1	-0.3	5.9	0	4.3
SR3	-4.5	-10	12.9	-1.6	-6.3	2.5
SR4	-2.9	-3.4	-6.9	-	-	-
SR5	2.4	-7.1	3.3	0	-7.1	-4.5
SR6	-2	0	-12.3	-0.3	-9.1	-13.1
Mean	**-0.2**	**-6.3**	**-1.1**	**0.6**	**-5.5**	**-2.9**

Table 3. Goodness-of-fit statistics for calibrated CN loss method.

Table 4 displays the Green and Ampt soil moisture parameters per watershed. Three soil classes were present across the watersheds, with loam based soils dominating, typical of a major floodplain location. Of note the range of saturated content (porosity) values was very small for all soil classes. When entering these values into the runoff model the output sensitivity was minimal compared to the CN loss method. Consequently the resulting goodness-of-fit statistics provided a better fit with the observed conditions for both storms per watershed (Table 5). All of the mean goodness-of-fit statistics fell within 2% with the largest individual errors occurring for SR5 for time to peak and difference in volume for both storms, and SR2 difference in peak for storm 2. Of note, the SR5 storms had no obvious skew present which suggests that the Green and Ampt soil conditions might require further calibration to match these particular storm distribution conditions. Nevertheless, the hydrograph errors were generally smaller than those generated from the CN loss method. Therefore the Green and Ampt method is the preferred method, providing that the necessary soil conditions can be measured or reliably estimated.

Watersheds	***Soil Class***	***Initial Content***	***Saturated Content***	***Suction (cm)***	***Hyd. Cond. (cm/hr)***
SR1	Loam	0.029	0.375-0.551	8.89	0.34
SR2, 5, 6	Silt Loam	0.015	0.420-0.582	16.68	0.65
SR3, 4	Sandy Loam	0.041	0.351-0.555	11.01	1.09

Table 4. Green and Ampt soil moisture parameters per watershed.

Watershed	***Storm 1***			***Storm 2***		
	Diff in Peak (%)	***Diff in time to peak (%)***	***Diff in volume (%)***	***Diff in Peak (%)***	***Diff in time to peak (%)***	***Diff in volume (%)***
SR1	-1.2	2.4	-2.1	2.3	1.1	-0.4
SR2	-0.3	1.8	-1.5	5.2	0.3	1.3
SR3	0.8	0.2	3.2	2.6	-0.1	0.7
SR4	0.4	0	0.8	-	-	-
SR5	1.2	5.6	4.2	-1.6	3.4	3.6
SR6	0.9	-0.7	-2.4	0.7	2.8	-0.9
Mean	**0.3**	**1.6**	**0.4**	**1.8**	**1.5**	**0.9**

Table 5. Goodness-of-fit statistics for Green and Ampt loss method.

In conclusion it appears that the empirical CN loss method is capable of accurately reproducing observed runoff for a range of storm intensities in comparison to the Green and Ampt method, although the CN method is more sensitive to both the distribution of the storm hyetograph and proportion of impervious cover. As a result, greater calibration is required when applying the CN method. If the necessary soil infiltration parameters are available or can be reliably estimated, the Green and Ampt method is preferred as it appears less sensitive to these same conditions.

Further research from this point would include applying these same methods to larger watersheds with more complex distributions of soil and land cover conditions to assess the sensitivity of both methods. Also, considering that this research focused on urban watersheds, future modeling research could incorporate the subterranean stormwater collection systems found in urban areas. The Storm Water Management Model (SWMM), for example, can incorporate both surface and subterranean flow as a dual-drainage approach to produce both a combined and split surface and subterranean hydrograph that one would typically expect in an urban watershed.

References

Dunne, T., and L. B. Leopold. 1978. *Water in Environmental Planning*. Freeman: San Francisco, CA.

Evaldi, R. D., and B. L. Moore. 1994. Techniques for estimating the quantity and quality of storm runoff from urban watersheds of Jefferson County, Kentucky. *Water-Resources Investigations Report 94-4023.* US Geological Survey: Louisville, KY.

Hawkins, R. H., T. J. Ward, D. E. Woodward, and J. A. Van Mullem. 2005. *Progress Report: ASCE Task Committee on Curve Number Hydrology. Managing Watersheds for Human and Natural Impacts*: pp. 1-12. doi: 10.1061/40763(178)150.

Hejazi, M. I., and M. Markus. 2009. Impacts of urbanization and climate variability on floods in northeastern Illinois. *Journal of Hydrologic Engineering* 14: 606-616.

Metropolitan Sewer District (MSD). 2016. Rainfall conditions for Jefferson County, Kentucky. Available at: http://www.msdlouky.org/aboutmsd/rain-info.html (last accessed Mar 5 2017).

National Oceanic and Atmospheric Administration (NOAA). 2015. NOAA Atlas 14 Point Precipitation Frequency Estimates: Ky. Available at: http://hdsc.nws.noaa.gov/hdsc/pfds/pfds_map_cont.html?bkmrk=ky (last accessed Sep12 2015).

Natural Resources Conservation Service (NRCS). 2016. Soils. Description of STATSGO2 Database. Available at: https://www.nrcs.usda.gov/wps/portal/nrcs/detail/soils/survey/geo/?cid=nrcs142p2_053629 (last accessed March 5 2017).

Rawls, W. J., D. L. Brakensiek, and N. Miller. 1983. Green–Ampt infiltration parameters from soils data. *Journal of Hydraulic Engineering* 109: 62–70.

US Department of Agriculture (USDA). 1986. Urban hydrology for small watersheds. *Technical Report 55*. USDA: Washington, DC.

US Geological Survey (USGS). 2016a. National Elevation Dataset (NED). Available at: https://lta.cr.usgs.gov/NED (last accessed Mar 5 2017).

US Geological Survey (USGS). 2016b. High Resolution Orthoimagery (HRO). Available at: https://lta.cr.usgs.gov/high_res_ortho (last accessed Mar 5 2017).

US Environmental Protection Agency (US EPA). 2003. Protecting water quality from urban runoff. *Fact Sheet 841-F-03-003.* US EPA: Washington, DC.

Van Mullem, J. A. 1991. Green Ampt and the curve number. *ASAE Paper 91-2610.* ASAE: Chicago, IL.

Dynamics of trace metal and ion concentrations in reclaimed mountaintop removal and reference headwater streams

Basic Information

Title:	Dynamics of trace metal and ion concentrations in reclaimed mountaintop removal and reference headwater streams
Project Number:	2016KY257B
Start Date:	3/1/2016
End Date:	2/28/2017
Funding Source:	104B
Congressional District:	KY 5th
Research Category:	Water Quality
Focus Category:	Hydrogeochemistry, Water Quality, Geochemical Processes
Descriptors:	None
Principal Investigators:	Steven John Price

Publications

1. Freytag, Sara B., 2016, Effects of Mountaintop Removal Mining on Population Dynamics of Stream Salamanders, MS Thesis, Department of Forestry, College of Agriculture Food and Environment, University of Kentucky, Lexington, KY, 94 p.
2. Price, Steven and Sara Freytag, 2017, Dynamics of Trace Metal and Ion Concentrations in Reclaimed Mountaintop Removal and Reference Headwater Streams, in Proceedings of the 2017 Water Resources Annual Symposium, Kentucky Water Resources Research Institute, Lexington, Kentucky, p. 59.

Dynamics of Trace Metal and Ion Concentrations in Reclaimed Mountaintop Removal and Reference Headwater Streams

Problem and Research Objectives

Mountaintop removal mining (MTR), a form of surface mining that involves the removal of significant amounts of rock to access shallow coal deposits, is a stressor of stream ecosystems throughout the Central Appalachia region of the eastern USA (Bernhardt & Palmer 2011; Wickham et al. 2013). Mountaintop removal mining often results in the complete or partial burial of low-order or headwater streams via valley-filling (VF), the process by which rock (i.e., overburden materials) is discarded from the mine site into adjacent valleys (Bernhardt & Palmer 2011). It is well known that VF alters stream water chemistry; leaching and surface runoff from the unweathered overburden materials leads to increased specific conductance and ion concentrations, elevated levels of total dissolved solids and some trace metals, and altered pH in comparison to reference streams (Palmer et al. 2010; Griffith et al. 2012). Such modifications to water chemistry likely contribute to diminished biological communities in MTR streams (Pond 2010; Muncy et al. 2014; Hitt & Chambers 2014).

To better understand dynamics of streams impacted by MTR and VF, recent proposals (i.e., the recently revoked Stream Protection Rule) stress the need for monitoring a comprehensive set of water quality parameters, which include both spatial and temporal replicates. The objectives of this study were to compare trace metal and ion concentrations in 11 valley-filled headwater streams (MTR-VF) and 12 reference headwater streams, located on the Laurel Fork surface mine and University of Kentucky's (UK) Robinson Forest, respectively. No changes were made to the original project proposal; however here we provide some year-to-year comparisons of select water quality variables to provide greater temporal resolution.

Methodology

We collected grab samples yearly from 2013, 2014, and 2015 and monthly from April 2015 to March 2016 at 11 MTR-VF streams located on Laurel Fork surface mine and 12 reference streams on UK's Robinson Forest in Breathitt and Knott Counties, KY (Fig. 1). All samples were brought to UK for water chemistry analysis. The following variables were analyzed in the UK's Forest Hydrology Lab using standard methods (Greenberg *et al.* 1992): specific conductance (µS/cm), pH [H+], {Ca, Cl, Fe, K, Mg, Mn, Na, NH_4-N, NO_2-N, NO_3-N, PO_4, SO_4} (mg/L), and total organic carbon (mg/L C).

Inductively Coupled Plasma spectroscopy (ICP) was conducted at the Environmental Research Training Laboratory. To test for total metals, samples were prepared using digestion method 3030 E; the rest of the procedure used method 3120 B (Greenberg *et al.* 1992). Elements evaluated included: {Ag, Al, As, Ba, Be, Cd, Co, Cr, Cu, Fe, Ni, Pb, Sb, Se, Tl, Y, Zn, (mg/L). included the following: {Ag, Ba, Be, Y at detection limit 0.001}, {Cd, Co, Cr, Cu, Ni, Pb, Sb, Zn at detection limit 0.005}, {As, Se, Tl at detection limit 0.01}, {Al, Fe at detection limit 0.05}. Analyses were completed in June 2016.

We use a mixed model with an autoregressive covariance structure (repeated measures ANOVA; SAS, v. 9.3) to compare site type means and dynamics from two time periods. First, we examined the effects of site type (i.e., reference vs. MTR-VF) and year on water quality variables (i.e., specific conductance, ions, pH and total organic carbon, see above) using data collected in May 2013, May 2014, and May 2015. Second, we evaluated the effects of site type and month on water quality variables (see above) and trace metals generated through coupled plasma spectroscopy. For all models, protected Least Significant Difference (LSD) post-hoc t-tests were conducted on significant interactions.

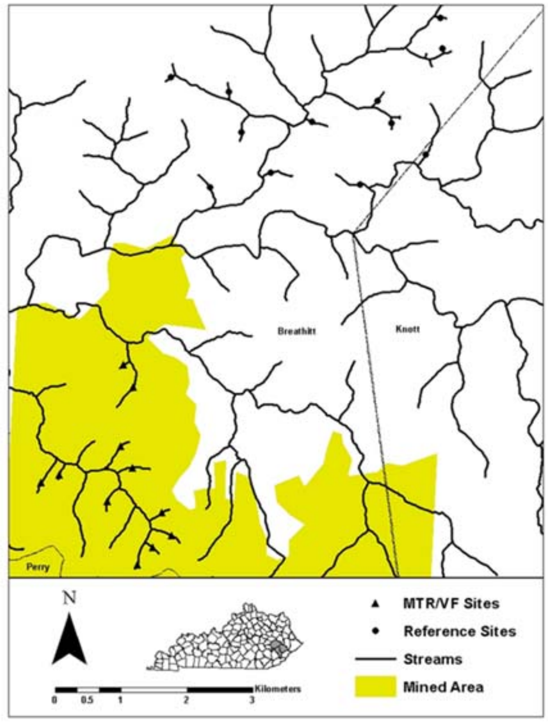

Fig. 1. We collected grab samples at 11 MTR-VF stream reaches, on the reclaimed Laurel Fork Surface Mine, and 12. Reference stream reaches on UK's Robinson Forest, Breathitt and Knott Counties, KY.

Principal Findings

Year-to-Year Comparison

Specific conductance, TOC, pH and most ion concentrations were significantly different between MTR-VF and reference stream reaches, varied among years, and showed an interaction between site type and year (Table 1). The interaction between site type and year was due primarily to the variability of ion concentrations in streams impacted by MTR-VF, which has substantial variance on mean values relative to the variance seen in reference sites (Table 1). For example, a comparison of specific conductance over the 3 years revealed a significant interaction of site type and year ($F (2, 42) = 24.04$, $p < 0.001$), with LSD post-hoc t-tests revealing that MTR-VF stream reaches were significantly different among years ($p<0.05$) while mean specific conductance of reference sites was not significantly different among years (Fig. 2).

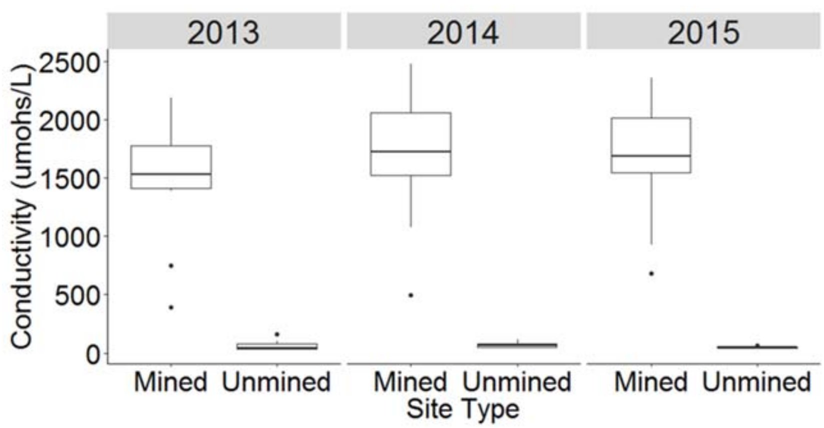

Fig. 2. Comparison of conductance from May 2013-2015 at 11 stream sites impacted by MTR-VF and 12 reference (i.e., unmined) sites.

Table 1. Most ions were significantly different between site types, among years, and showed an interaction between site type and year. Significance is shown as p-values below column headings for each water chemistry variable. Ranges depict the minimum and maximum values of the water chemistry variables recorded from May 2013-2015.

Variable	Site Type	Year	Year x Site Type	Range MTR-VF	Range Ref.
Conductivity (umohs/L)	< 0.0001	0.0001	0.0003	389-2480	27.5-157.3
TOC (mg/L C)	0.0075	0.0795	0.5786	1.74-31.69	1.13-20.34
PO4 (mg/L)	0.1609	0.1223	0.1426	0-0.09	0-1.36
pH[H+]	0.0031	< 0.0001	0.0026	4.34-8.33	3.47-7.08
Mn (mg/L)	< 0.0001	0.0079	0.0083	0.03-13.75	0-0.04
Cl (mg/L)	0.3654	0.035	0.7919	0.31-1.57	0.3-0.8
SO4 (mg/L)	< 0.0001	0.6683	0.6683	8.45-1295.56	2.68-20.17
NO3-N (mg/L)	0.9632	0.0044	0.0622	0-2.83	0-2.26
NH4-N (mg/L)	0.2137	0.0072	0.6854	0-0.61	0-0.84
Ca (mg/L)	< 0.0001	< 0.0001	< 0.0001	16.94-60.83	0.72-5.16
Mg (mg/L)	< 0.0001	< 0.0001	< 0.0001	8.8-20.57	1.06-2.96
K (mg/L)	< 0.0001	0.0075	0.1915	2.89-15.29	1.07-11.96
Na (mg/L)	< 0.0001	0.0001	< 0.0001	3.55-17.84	0.71-9.1
NO2-N (mg/L)	0.0018	< 0.0001	0.0004	0-0.8	0-0.18
Fe (mg/L)	0.0966	0.0722	0.0735	0-8.96	0-0.02

Month-to-Month Comparison

We found significant differences between MTR-VF and reference stream reaches, among months and an interaction between site type and month for specific conductance, TOC, pH and ion concentrations (Table 2). Similar to the year-to-year comparison, we found that ion concentrations were dynamic across both site types; however, the maximum ion concentrations on MTR-VF sites were often greater than those at reference sites (Table 2, Fig. 3).

Although some of the trace metal concentrations assessed were at or below the detection limit (i.e., As, Cd), several of the trace metals were significantly different between sites types, among months and showed an interaction between site type and month. Again, the ranges indicate that trace metal concentrations vary spatially and temporally (often ranging from below to above the detection limits) in both site types. However, the concentrations at MTR-VF sites were often greater than those at reference sites, particularly values for Al, Ni, Se and Y (Fig. 4).

Significance

Our results indicate that water chemistry variables in MTR-VF streams and reference streams show substantial variation between site types and among years and months. In particular, streams impacted by MTR-VF were particularly dynamic. Although few studies have assessed water chemistry dynamics in MTR-VF streams, Green et al. (2000; US EPA) found mean conductivity greatest in the summer likely due to reduced discharges. Our data show similar patterns (at least in June and July), although future research should examine the relationship between discharge, precipitation and ion concentrations. The dynamics of both trace metals and ion concentrations highlight the need for more intensive temporal monitoring of stream water chemistry in Central Appalachia. Extensive monitoring efforts may be required to elucidate the precise mechanism behind reduced biological communities in streams impacted by

Table 2. All ions surveyed were significantly different between site types, among months, and showed an interaction between site type and month. Significance is shown as p-values below column headings for each water chemistry variable. Ranges depict the minimum and maximum values of the water chemistry variables recorded from April 2015 to March 2016.

Variable	Site Type	Month	Month x Site Type	Range MTR-VF	Range Ref.
Conductivity (umohs/L)	< 0.0001	< 0.0001	< 0.0001	81.4-2690	25.7-101.5
TOC (mg/L C)	0.0014	< 0.0001	< 0.0001	1.26-44.37	0.73-7.79
PO4 (mg/L)	0.0383	< 0.0001	0.0065	0-2.52	0-2.5
pH[H+]	< 0.0001	< 0.0001	0.0023	3.72-8.06	4.23-6.61
Mn (mg/L)	0.0002	< 0.0001	< 0.0001	0-14.89	0-0.17
Cl (mg/L)	0.0103	< 0.0001	< 0.0001	0.22-8.15	0.25-1.42
SO4 (mg/L)	< 0.0001	0.0002	0.0003	5.59-1647.09	4.95-599
NO3-N (mg/L)	< 0.0001	< 0.0001	< 0.0001	0-0.48	0-1.22
NH4-N (mg/L)	< 0.0001	< 0.0001	< 0.0001	0-1.26	0-0.7
Ca (mg/L)	< 0.0001	< 0.0001	< 0.0001	26.5-120.35	0.67-7.89
Mg (mg/L)	< 0.0001	< 0.0001	< 0.0001	5.15-22.38	0.69-4.13
K (mg/L)	< 0.0001	< 0.0001	< 0.0001	1.54-11.51	0.75-4.15
Na (mg/L)	< 0.0001	< 0.0001	< 0.0001	2.37-25.54	0.52-5.27
NO2-N (mg/L)	< 0.0001	< 0.0001	< 0.0001	0-1.54	0-0.54
Fe (mg/L)	0.0326	0.0125	0.0264	0-18.37	0-0.63

MTR-VF, and ultimately provide guidance for restoration efforts.

Table 3. Several trace metals surveyed were significantly different between site types, among months, and showed an interaction between site type and month. Significance is shown as p-values below column headings for each water chemistry variable. Ranges depict the minimum and maximum values of the water chemistry variables recorded from April 2015 to March 2016.

Variable (mg/L)	Site Type	Month	Site Type x Month	Range MTR-VF	Range Ref.
Ag	< 0.001	< 0.001	< 0.001	0.001-0.004	0.001-0.002
Al	0.006	0.037	0.015	0.019-18.079	0.02-2.51
As	*at or below detection limit			0.01-0.02	0.01-0.02
Ba	0.001	0.0021	0.138	0.008-0.044	0.015-0.236
Be	0.002	0.055	0.097	0.001-0.0127	0.001-0.005
Cd	*at or below detection limit			0.003-0.005	0.003-0.005
Co	0.0009	< 0.0001	0.1669	0.005-0.113	0.005-0.025
Cr	0.3089	< 0.0001	0.3693	0.0015-0.01	0.005-0.01
Cu	0.8541	< 0.0001	0.5975	0.002-0.087	0.002-0.141
Fe	0.0079	0.1627	0.646	0.036-14.294	0.051-3.66
Ni	0.0008	< 0.001	0.001	0.008-0.276	0.006-0.02
Pb	0.0162	< 0.001	0.001	0.005-0.008	0.005-0.005
Sb	< 0.001	< 0.001	< 0.001	0.005-0.033	0.005-0.03
Se	< 0.001	< 0.001	< 0.001	0.005-0.025	0.005-0.01
Tl	0.0087	< 0.001	0.0041	0.01-0.05	0.01-0.05
Y	0.0051	0.0026	< 0.001	0.001-0.09	0.001-0.005
Zn	0.004	< 0.001	0.022	0.002-0.37	0.002-0.204

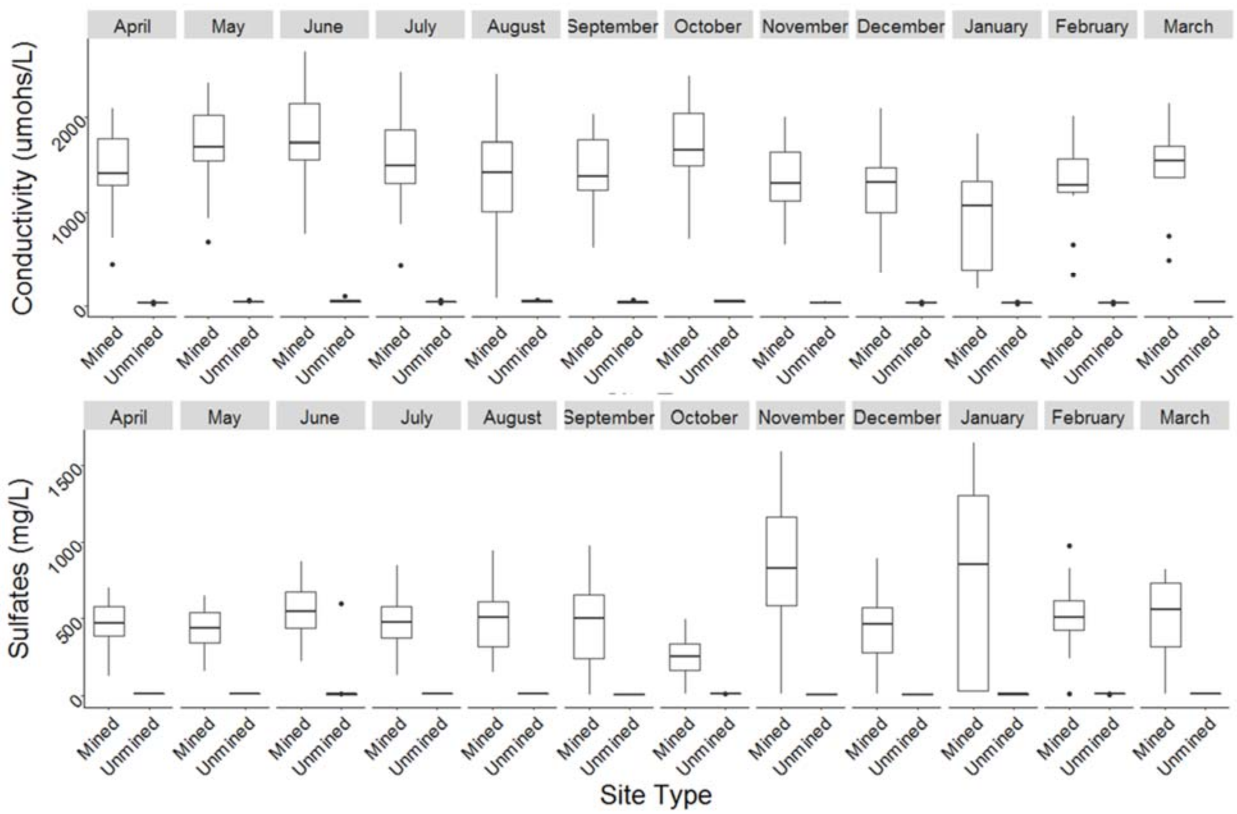

Fig. 3. For April 2015-March 2016 water samples, there was a significant interaction between site type and month ($F(11,229)=11.70$, $p<0.0001$; $F(11,229)=3.32$, $p<0.0003$) for both specific conductance and sulfates.

References

Bernhardt, E.S., and M.A. Palmer. 2011. The environmental costs of mountaintop mining valley fill operations for aquatic ecosystems of the Central Appalachians. Ann. N.Y. Acad. Science. 1223:39-57.

Green J., M. Passmore, and H. Childers. A survey of the conditions of stream in the primary region of mountaintop mining/valley fill coal mining. Mountaintop mining/valley fills in Appalachia. Final programmatic environmental impact statement. Philadelphia, PA: U.S. Environmental Protection Agency, Region 3; 2000. Appendix D. Available from http://www.epa.gov/Region3/mtntop/pdf/appendices/d/streamsinvertebrate-study/FINAL.pdf.

Griffith, M.B., Norton, S.B., Alexander, L.C., Pollard, A.I., and S.D. Leduc. 2012. The effects of mountaintop mines and valley fills on the physicochemical quality of stream ecosystems in the central Appalachians: A review. Science of the Total Environment 417-418: 1-12.

Hitt, N.P., and D.B. Chambers. 2014. Temporal changes in taxonomic and functional diversity of fish assemblages downstream from mountaintop mining. Freshwater Science 33: 915-926.

Muncy, B.L., Price, S.J., Bonner, S.J., and C.D. Barton. 2014. Mountaintop removal mining reduces stream salamander occupancy and richness in southeastern Kentucky (USA). Biological Conservation 180: 115-121.

Palmer, M.A., Bernhardt, E.S., Schlesinger, W.H., Eshleman, K.N., Foufoula-Georgious, E., Hendryx, M.S., Lemly, A.D., Likens, G.E., Loucks, O.L., Power, M.E., White, P.S., and P.R. Wilcock. 2010. Mountaintop mining consequences. Science 327:148-149.

Pond, G.J. 2010. Patterns of Ephemeroptera taxa loss in Appalachian headwater streams (Kentucky, USA). Hydrobiologia 641**:** 185-201.

Wickham, J., Bohall Wood, P., Nicholson, M.C., Jenkins, W., Druckenbrod, D., Suter, G.W., Strager, M.P., Mazzarella, C., Galloway, W., and J. Amos. 2013. The overlooked terrestrial impacts of mountaintop mining. Bioscience 63: 335-348.

Sediment fingerprinting and biogeochemical erosional model of the Otter Creek Basin, Fort Kox Army Post, Kentucky

Basic Information

Title:	Sediment fingerprinting and biogeochemical erosional model of the Otter Creek Basin, Fort Kox Army Post, Kentucky
Project Number:	2016KY258B
Start Date:	3/1/2016
End Date:	2/28/2017
Funding Source:	104B
Congressional District:	KY 2nd
Research Category:	Climate and Hydrologic Processes
Focus Category:	Geomorphological Processes, Sediments, Surface Water
Descriptors:	None
Principal Investigators:	Alan Fryar

Publication

1. Peterman, Cara L., Alan Fryar, and Dwayne Edwards, 2017, Soil and Sediment Fingerprinting of the Otter Creek Watershed Draining Fort Knox: An Advanced Game of Match, in Proceedings of the 2017 Kentucky Water Resources Annual Symposium, Kentucky Water Resources Research Institute, Lexington, Kentucky, p. 65-66.

Sediment Fingerprinting and Biogeochemical Erosional Model of the Otter Creek Basin, Fort Knox Army Post, Kentucky

Problem and Research Objectives

The objectives of this study were to (1) characterize the extent of erosion within the Otter Creek drainage area and spatially determine sources of sediment inputs to the creek; (2) assess the impact of subsequent restoration efforts from training areas using stable C and N isotopes and the C/N atomic ratio to investigate the spatial erosional processes within the sub-watershed of Otter Creek on Fort Knox Army Post; and (3) utilize a multivariate unmixing model and the geochemical composition of the sediment sources within the training areas to identify contributing sources.

Methodology

Time-integrated sediment samplers (Phillips et al. 2000) were placed at three locations along Otter Creek (Figure 1), where they collected fine sediment (< 53 μm) transported from upland areas. Sampling site 1 was located as Otter Creek enters Fort Knox, sampling site 3 as the creek leaves Fort Knox, and sampling site 2 about halfway between sites 1 and 2. To ensure that the sediment traps were placed correctly, stream velocity profiles were measured at each of the three sampling sites using a SonTek Handheld-ADV FlowTracker. Flow depths and velocities were measured just upstream from each proposed sampling location at baseflow conditions. The sediment traps were placed within the high-velocity areas to capture as much sediment as possible. Each week, the samplers were emptied for sediment analyses and clean traps were put into place. Sediment collected during the 56-week study is being analyzed for bulk carbon (total, inorganic, and organic) and nitrogen, carbon and nitrogen isotopes ($\delta^{13}C$ and $\delta^{15}N$, respectively, where the δ notation refers to the relative abundance of the stable isotope of interest), and grain size.

Soil samples have been collected from the training areas at Fort Knox and from residential and agricultural areas. Samples collected were split into two: one set was freeze-dried, ground and sieved for C and N isotope analysis; the other was processed for grain-size analysis.

At sites 1 and 2, In-Situ dataloggers were installed for nearly 11 months and were recording stream pH, temperature, and electrical conductivity (EC) at 15-minute intervals. The data have been downloaded and are being analyzed. Lastly, water-quality parameters (pH, temperature, EC, and dissolved oxygen) were monitored manually each week with a YSI 556 multi-parameter meter and probes.

A subset of samples was sent to the University of Chicago for preliminary stable isotope analyses in January 2016. This enabled us to determine how much sample was needed to distinguish $\delta^{13}C$ and $\delta^{15}N$ signals. All samples are now being analyzed in the University of Kentucky's Department of Earth and Environmental Sciences stable isotope lab using a Costech ECS 4010 elemental analyzer.

Because the geology of the Fort Knox area is dominated by carbonate rocks, inorganic carbon (IC) will be present in sediment samples and must be accounted for to quantify organic carbon (OC) by difference (OC = total C – IC). Coulometric analyses of C in sediment samples were performed at the Kentucky Geological Survey.

Grain-size analysis for sediment is being performed using a SediGraph particle-size analyzer, while soil samples are being analyzed for grain size using a LISST portable laser-diffraction particle-size analyzer.

Principal Findings and Significance

Sediment is one of the primary nonpoint source pollutants in surface waters (Davis and Fox 2009). Sediment fingerprinting and soil erosion models are valuable tools in identifying provenance and redistribution of sediment in a complex spatial and temporal setting such as Fort Knox and adjoining rural areas. The preliminary findings of this study help demonstrate the roles of seasonal changes, restoration efforts, and land use in the transport of fine particulate organic C and N. In addition, a roughly 1.6-km section of Otter Creek disappears into a subsurface conduit under baseflow conditions, which could influence IC values for sites 2 and 3.

Erosion of soil involves the process of detachment of particles from the soil surface and their transport by rainfall and runoff (Mahabaleshwara and Nagabhushan 2014). In the Otter Creek area, tracked-vehicle training, agricultural activities and subsequent rainfall or freeze/thaw prompt an increase in erosion.

We initially hypothesized that the sources of sediment were primarily from military training. While analyses are ongoing, preliminary results suggest that there are differences in the $\delta^{13}C$ and $\delta^{15}N$ signatures of soil and sediment, indicating that the rural area surrounding Fort Knox might contribute significant amounts of sediment.

Figure 2 shows the relationship between total C and N percentages at the three sites along Otter Creek. In general, N increases with C. Site 1 drains primarily agricultural and residential lands, which is reflected in generally higher C and N values, while site 3 drains training areas with soils that have been leached and eroded, therefore imparting sediment that tends to have lower amounts of C and N. Though only samples from October through the beginning of March have been analyzed thus far, as seen in Figures 3 and 4, both $\delta^{13}C$ and $\delta^{15}N$ demonstrate seasonality, showing a downward trend during the winter months. Samples for the summer and fall of 2016 are being analyzed, but we anticipate that $\delta^{13}C$ and $\delta^{15}N$ values will increase during those months.

Analysis of sediment samples for OC and IC demonstrated a seasonal variability, with lower amounts seen during summer months. This could be due to warmer water temperatures and the lower availability of dissolved oxygen (Figure 5), in addition to fluctuating precipitation events (Figure 6). In addition, there is a slight distinction seen among the sampling sites for dissolved oxygen and temperature, which could be attributed to source contributions.

Total carbon values for both military training and nonmilitary areas varied between the two, as nonmilitary areas are not as heavily eroded and exposed as the military training lands that drain to Otter Creek. IC values were so low in both sets of soil samples that they were unable to be detected by the coulometric analysis. Therefore, soil TC values essentially represent OC.

As noted above, soil and sediment analyses are ongoing. However, initial data have shown some minor distinctions between each of the sampling locations along Otter Creek and between military and nonmilitary upland source areas. As additional data are analyzed, the use of a sediment fingerprinting approach will help quantify the primary sources of sediment within Otter Creek, and provide useful information on the implementation of a stream or watershed rehabilitation approach for both Fort Knox and local communities.

Figures

Figure 1: Study-area map showing sediment-sampler locations and sub-watershed boundaries.

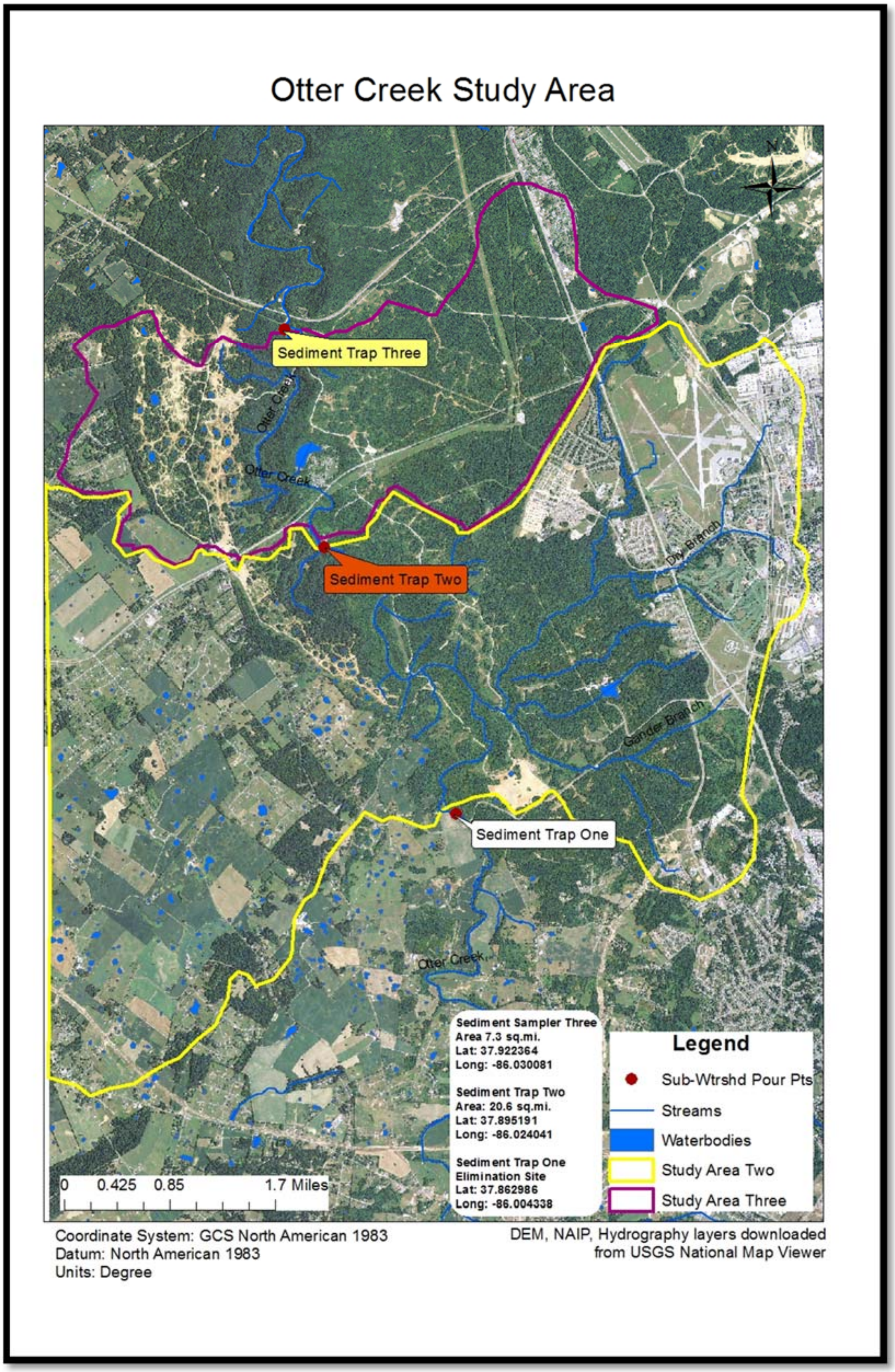

Figure 2: Percent carbon and nitrogen by sample site.

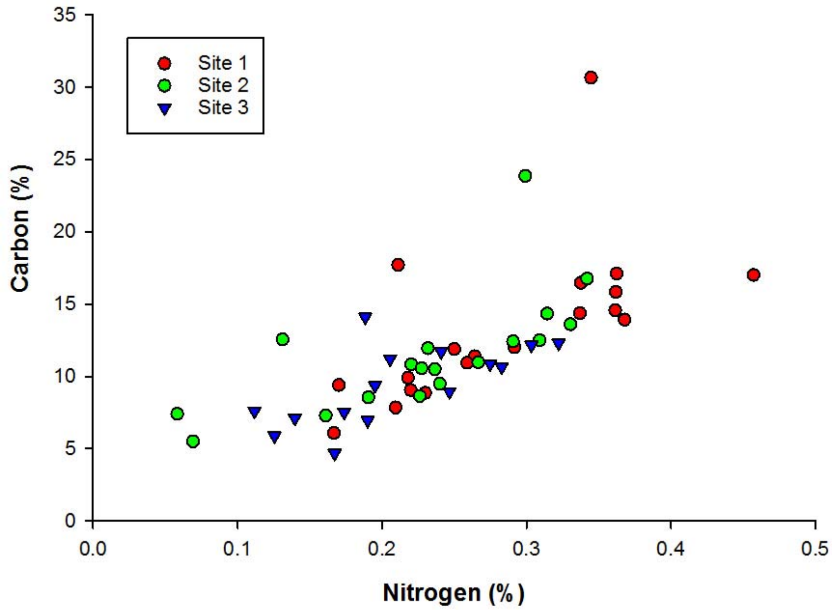

Figure 3: $\delta^{13}C$ of sediment, October 2015 – March 2016.

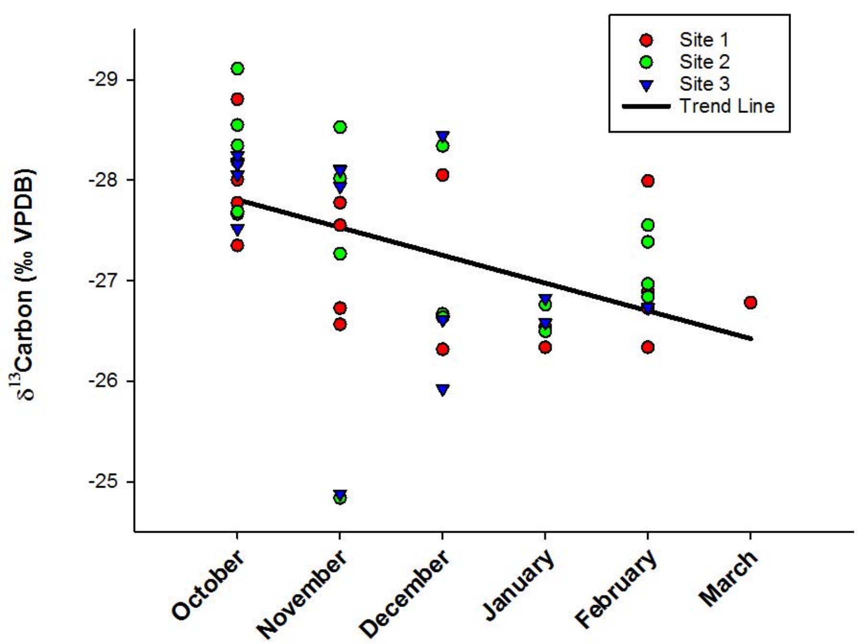

*Figure 4***:** δ^{15}N of sediment, October 2015 – March 2016.

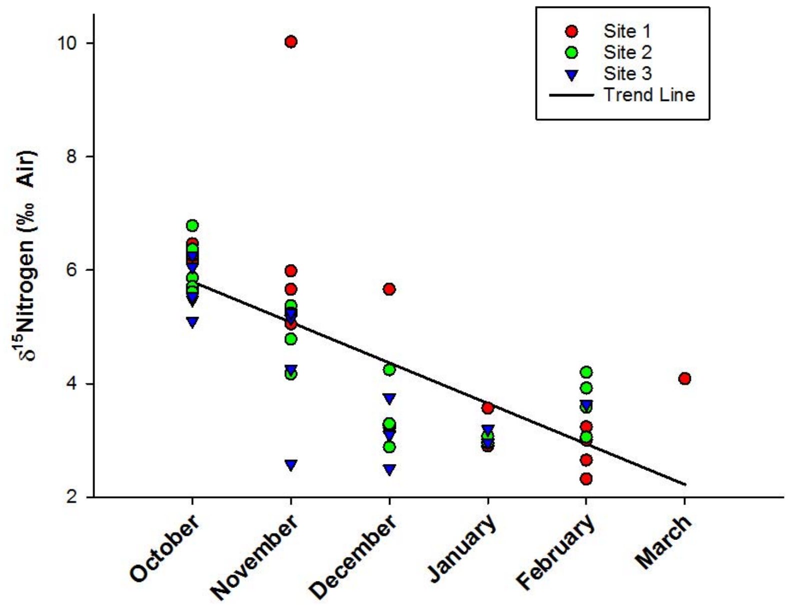

Figure 5: Temperature and dissolved oxygen values by site.

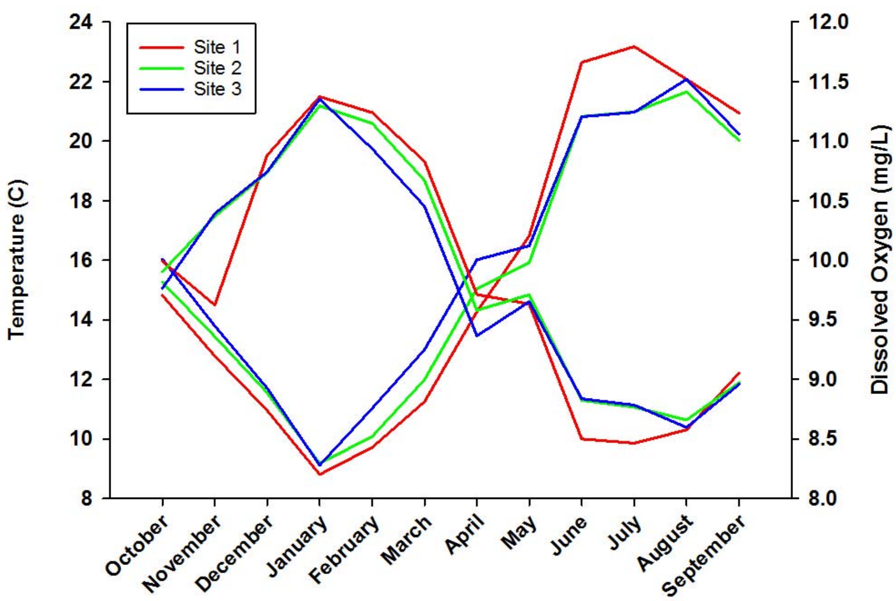

Figure 6: Monthly total precipitation at Ft. Knox during the study.

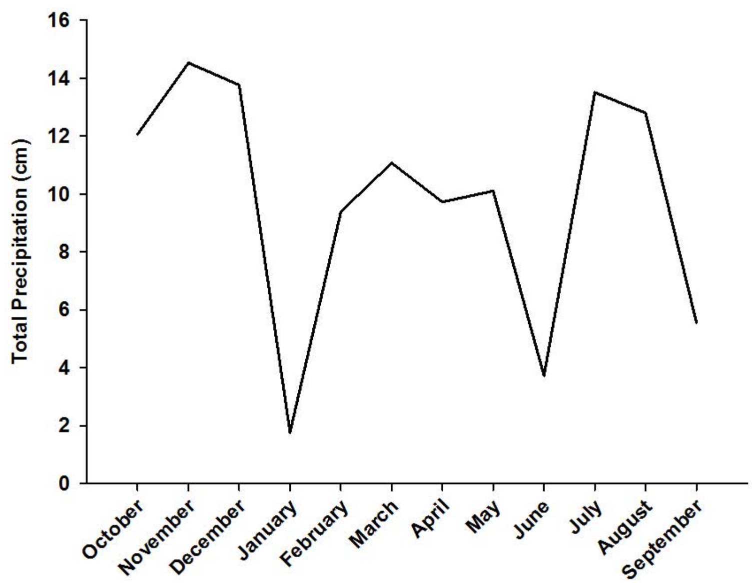

Works Cited

Davis, Charles M., and James F. Fox. 2009. "Sediment Fingerprinting: Review of the Method and Future Improvements for Allocating Nonpoint Source Pollution." *Journal of Environmental Engineering* (135): 490-504.

Mahabaleshwara, H, and H.M. Nagabhushan. 2014. "A Study on Soil Erosion and its Impacts on Floods and Sedimentation." *International Journal in Research in Engineering and Technology* 3 (3): 443-450.

Phillips, J.M., M.A. Russell, and D.E. Walling. 2000. "Time-integrated sampling of fluvial suspended sediment: a simple methodology for small catchments." *Hydrological Processes* 14: 2589-2602.

Bankfull regional curves and hydraulic geometry for the Eastern Kentucky Coal Field

Basic Information

Title:	Bankfull regional curves and hydraulic geometry for the Eastern Kentucky Coal Field
Project Number:	2016KY259B
Start Date:	3/1/2016
End Date:	2/28/2017
Funding Source:	104B
Congressional District:	KY 5th
Research Category:	Climate and Hydrologic Processes
Focus Category:	Floods, Surface Water, Geomorphological Processes
Descriptors:	None
Principal Investigators:	Carmen Agouridis

Publications

1. Berry, Ashlan, 2016, Development of Regional and Hydraulic Geometry Curves for the Eastern Kentucky Coalfields, MS Thesis, Department of Biosystems and Agricultural Engineering, College of Agriculture Food and Environment, University of Kentucky, Lexington, Kentucky, 257 p.
2. Berry, Ashlan and Carmen Agouridis, 2017, Bankfull Regional Curves and Hydraulic Geometry Curves for the Eastern Kentucky Coalfields, in Proceedings of the 2017 Kentucky Water Resources Annual Symposium, Kentucky Water Resources Research Institute, Lexington, Kentucky, p. 3-4.

Bankfull Regional Curves and Hydraulic Geometry Curves
for the Eastern Kentucky Coalfields

Problem and Research Objectives

Bankfull regional curves which relate bankfull channel dimensions (e.g. area, width, depth, discharge) to drainage area as well as hydraulic geometry curves that use bankfull discharge as the independent variable are useful tools for assisting in the correct identification of bankfull. Regional curves are particularly helpful when assessing incised stream systems where lack of good bankfull indicators is a common and problematic occurrence. To obtain the necessary information to develop regional and hydraulic geometry curves, data must be acquired from several reference regional streams representing a wide range of drainage areas (and bankfull discharges), a task that is often viewed as cost prohibitive for most project budgets. Designers not equipped with regional and hydraulic geometry curves face increased risks in misidentifying bankfull or using an incorrect return interval (e.g. 1.5-year event may be too large or too small for a specific region), and hence designing a channel with inappropriate dimensions. With increased demand for stream restoration (mitigation) projects in the eastern Kentucky Coalfields (EKC) due to current and historic mining activities (e.g. data needs of U.S. Army Corps of Engineers, U.S. Environmental Protection Agency, Kentucky Division of Water) and the expansion of the Mountain Parkway (e.g. data needs of Kentucky Transportation Cabinet) the demand for regional and hydraulic geometry curves applicable to this hydro-physiographic region is high. Such curves could be widely disseminated through research publications and Stream Stats version 3, much like the curves developed by Brockman et al. (2012) for the Inner and Outer Bluegrass regions of Kentucky.

The EKC contains five hydrologic landscape regions (HLRs) though only three were examined in this study: HLRs 9, 11 and 16 (HLRs 4 and 6 were too small). HLR 9 is characterized as having “humid plateaus with impermeable soils and permeable bedrock” (Wolock et al., 2004); it is predominately located in the western portion of the EKC. HLR 9 has overland flow and deep ground water as well as moderate regions of karst landscape. About 10% of the EKC is classified as HLR 9. HLR 11 is characterized as having “humid plateaus with impermeable soils and bedrock” (Wolock et al., 2004). Covering 40% of the EKC, HLR 11 is similar to 9 except the bedrock of HLR 11 is impermeable while it is permeable with HLR 9. Overland flow is predominating in HLR 11. HLR 11 is located primarily in between HLRs 9 and 16. HLR 16 is defined as “humid mountains with permeable soils and impermeable bedrock” (Wolock et al., 2004). The terrain of HLR 16 is steeper than that of HLRs 9 and 11; like HLR 11, the bedrock is impermeable but unlike either HLR 9 or 11, the soils are deemed permeable though shallow. Because of the permeable soils, HLR 16 has shallow groundwater flow. HLR 16 covers the biggest portion of EKC at 47%.

The purpose of this work was to develop regional and hydraulic geometry curves for the eastern Kentucky Coalfields. The specific objectives of the project were to:

- Determine bankfull recurrence intervals and develop regional and hydraulic geometry curves for the EKC
- Develop and compare regional and hydraulic geometry curves for hydrologic landscape regions 9, 11, and 16 in the EKC
- Compare these curves to theoretical values and results from other such curves developed in the U.S.

Data collection (e.g. geomorphic surveys, USGS discharge data) and analysis occurred during the spring and summer of 2016.

Methodology

Development of regional and hydraulic geometry curves followed the methodology outlined in Brockman et al. (2012) and Agouridis et al. (2011). Briefly, all U.S. Geological Survey (USGS) gage stations within the region with at least 10 years of discharge data were identified. Google Earth was used to inspect these sites for lack of tributaries entering near the gaging stations as well as potential issues with accessibility. Field visits were conducted to further evaluate the suitability of each site with respect to meeting established criteria (Brockman et al., 2012; Agouridis et al., 2011). The HLR for each gage was identified using ArcGIS.

Guidelines established by Harrelson et al. (1994) were used to collect the following field data at each selected site: representative riffles (goal of two per site), longitudinal profiles (20-30 bankfull widths), and pebble counts. Sinuosity was computed by using satellite images and ArcGIS. Streams were classified according to the Rosgen stream classification system (Rosgen, 1994). For active gages, bankfull discharges were computed using the Log Pearson Type III method as outlined in the USGS Bulletin 17B *Guidelines for Determining Flood Flow Frequency* (1982). Manning's n was computed for each riffle cross-section provided bankfull discharge data were available. Streamside vegetation (forest, grass, mixture of forest and grass) types were noted (Hession et al., 2003).

Cross-sectional (e.g. entrenchment ratio, width-to-depth ratio) and bed material (e.g. D_{50}) data were analyzed using RIVERMorph® software. Local bankfull slope values were computed using Microsoft Excel. Power functions were developed in Microsoft Excel for both regional and hydraulic geometry curves (Leopold et al., 1964). Regional and hydraulic geometry curves were created for all HLRs combined (e.g. HLRs 9, 11 and 16) as well as each individual HLR. For regional curves, the bankfull parameters cross-sectional area, width, mean depth, and discharge were the dependent variables while drainage area was the independent variable. For hydraulic geometry curves, the bankfull parameters cross-sectional area, width, mean depth, velocity, local slope, and Manning's n were the dependent variables while bankfull discharge was the independent variable.

Analyses of covariance (ANCOVAs) were performed in the statistical software package SAS version 9.4 using PROC REG. Regional and hydraulic geometry curves for each bankfull parameter within each HLR were compared (e.g. bankfull cross-sectional area for HLR 9 vs. bankfull cross-sectional area for HLR 11, bankfull cross-sectional area for HLR 9 vs. bankfull cross-sectional area for HLR 16, bankfull cross-sectional area for HLR 11 vs. bankfull cross-sectional area for HLR 16). Comparisons were also made between individual HLRs to the combined regional curves (e.g. bankfull cross-sectional area for HLR 9 vs bankfull cross-sectional area for HLRs 9, 11 and 16 combined) to determine if subdivision of a physiographic region based on HLR significantly improved the resultant regional and hydraulic geometry curves. Additionally, the regional and hydraulic geometry curves for each HLR were compared to U.S.-wide HLR-based regional curves, for instances when drainage area was less than or equal to 250 mi^2, developed by Blackburn-Lynch (2015). The bankfull parameters local slope and Manning's n from the individual and combined HLRs were not compared to the U.S.-wide HLRs as Blackburn-Lynch (2015) did not provide information on the bankfull parameters local slope and Manning's n. The coefficient of determination (R^2) was used to classify each fit as strong ($R^2 \geq 0.9$), good ($R^2 \geq 0.75$), moderate ($R^2 \geq 0.5$), and poor ($R^2 < 0.5$).

Principal Findings and Significance

Bankfull regional curves were created for each assessed stream in the entire EKC region, using stream morphology data from 47 sites relating bankfull parameters (discharge, cross-sectional area, width, and mean depth) to drainage area (Tables 1-4). Regional curves were also created for each evaluated individual HLR region (HLR 9, HLR 11, and HLR 16) within the EKC region.

Table 1: Bankfull regional curve relationships for bankfull discharge ($ft^3\ s^{-1}$) and drainage area (mi^2).

HLR	Regression Equation	R^2
Combined HLRs (9, 11 and 16)	$Q_{bkf}=37.54DA^{0.77}$	0.87
HLR 9	$Q_{bkf}=16.14DA^{0.90}$	0.88
HLR 11	$Q_{bkf}=54.49DA^{0.62}$	0.80
HLR 16	$Q_{bkf}=34.88DA^{0.92}$	0.97

Table 2: Bankfull regional curve relationships for bankfull cross-sectional area (ft^2) and drainage area (mi^2).

HLR	Regression Equation	R^2
Combined HLRs (9, 11 and 16)	$A_{bkf}=10.59DA^{0.74}$	0.94
HLR 9	$A_{bkf}=10.90DA^{0.76}$	0.91
HLR 11	$A_{bkf}=12.63DA^{0.69}$	0.94
HLR 16	$A_{bkf}=9.81DA^{0.76}$	0.95

Table 3: Bankfull regional curve relationships for bankfull width (ft) and drainage area (mi^2).

HLR	Regression Equation	R^2
Combined HLRs (9, 11 and 16)	$w_{bkf}=12.16DA^{0.42}$	0.91
HLR 9	$w_{bkf}=13.32DA^{0.42}$	0.97
HLR 11	$w_{bkf}=14.11DA^{0.38}$	0.92
HLR 16	$w_{bkf}=11.18DA^{0.42}$	0.90

Table 4: Bankfull regional curve relationships for bankfull mean depth (ft) and drainage area (mi^2).

HLR	Regression Equation	R^2
Combined HLRs (9, 11 and 16)	$d_{bkf}=0.88DA^{0.32}$	0.82
HLR 9	$d_{bkf}=0.82DA^{0.34}$	0.65
HLR 11	$d_{bkf}=0.89DA^{0.31}$	0.83
HLR 16	$d_{bkf}=0.89DA^{0.33}$	0.89

Hydraulic geometry curves relating bankfull parameters cross-sectional area, width, mean depth, velocity, local slope, and Manning's n to discharge were created for the entire EKC region (HLR 9, 11 and 16 combined) and each individual HLR region examined in the study (HLR 9, 11 and 16 separately) (Tables 5-10). Due to the low number of available active USGS gaged sites, only 24 of the 47 sites (51%) were used: 4 in HLR 9, 11 in HRL 11 and 9 in HLR 16.

Table 5: Hydraulic geometry curves for bankfull area (A_{bkf}). A_{bkf} is in units of ft^2 and Q_{bkf} is in units of $ft^3\ s^{-1}$.

HLR	Regression Equation	R^2
Combined HLR (9, 11 and 16)	$A_{bkf}=0.47Q_{bkf}^{0.92}$	0.96
HLR 9	$A_{bkf}=1.69Q_{bkf}^{0.77}$	0.99
HLR 11	$A_{bkf}=0.65Q_{bkf}^{0.88}$	0.97
HLR 16	$A_{bkf}=0.34Q_{bkf}^{0.93}$	0.99

Table 6: Hydraulic geometry curves for bankfull width (w_{bkf}). w_{bkf} is in units of ft and Q_{bkf} is in units of $ft^3\ s^{-1}$.

HLR	Regression Equation	R^2
Combined HLR (9, 11 and 16)	$w_{bkf}=2.56Q_{bkf}^{0.48}$	0.85
HLR 9	$w_{bkf}=4.96Q_{bkf}^{0.41}$	0.81
HLR 11	$w_{bkf}=4.09Q_{bkf}^{0.42}$	0.79
HLR 16	$w_{bkf}=1.97Q_{bkf}^{0.50}$	0.92

Table 7: Hydraulic geometry curves for bankfull mean depth (d_{bkf}). d_{bkf} is in units of ft and Q_{bkf} is in units of $ft^3\ s^{-1}$.

HLR	Regression Equation	R^2
Combined HLR (9, 11 and 16)	$d_{bkf}=0.19Q_{bkf}^{0.43}$	0.87
HLR 9	$d_{bkf}=0.35Q_{bkf}^{0.35}$	0.62
HLR 11	$d_{bkf}=0.16Q_{bkf}^{0.46}$	0.88
HLR 16	$d_{bkf}=0.17Q_{bkf}^{0.43}$	0.95

Table 8: Hydraulic geometry curves for bankfull velocity (v_{bkf}). v_{bkf} is in units of ft s^{-1} and Q_{bkf} is in units of ft^3 s^{-1}.

HLR	Regression Equation	R^2
Combined HLR (9, 11 and 16)	$v_{bkf}=2.11Q_{bkf}^{0.08}$	0.16
HLR 9	$v_{bkf}=0.59Q_{bkf}^{0.23}$	0.88
HLR 11	$v_{bkf}=1.55Q_{bkf}^{0.12}$	0.43
HLR 16	$v_{bkf}=2.92Q_{bkf}^{0.07}$	0.35

Table 9: Hydraulic geometry curves for bankfull slope (S_{bkf}). S_{bkf} is in units of ft ft^{-1} and Q_{bkf} is in units of ft^3 s^{-1}.

HLR	Regression Equation	R^2
Combined HLR (9, 11 and 16)	$S_{bkf}=0.06Q_{bkf}^{-0.49}$	0.27
HLR 9	$S_{bkf}=0.00Q_{bkf}^{0.04}$	1.00
HLR 11	$S_{bkf}=0.09Q_{bkf}^{-0.58}$	0.34
HLR 16	$S_{bkf}=0.02Q_{bkf}^{-0.13}$	0.25

Table 10: Hydraulic geometry curves for Manning's n at bankfull (n_{bkf}). n_{bkf} is dimensionless. Q_{bkf} is in units of ft^3 s^{-1}.

HLR	Regression Equation	R^2
Combined HLR (9, 11 and 16)	$n_{bkf}=0.07Q_{bkf}^{-0.07}$	0.07
HLR 9	$n_{bkf}=0.15Q_{bkf}^{0.23}$	1.00
HLR 11	$n_{bkf}=0.10Q_{bkf}^{-0.14}$	0.14
HLR 16	$n_{bkf}=0.04Q_{bkf}^{0.05}$	0.06

Results indicated that separating the EKC into HLRs improved the R^2 of the regional curves. Statistical differences were noted between HLRs with regards to regional curves further suggesting subdivision is beneficial. For hydraulic geometry curves, lack of discharge data limited interpretations and hence recommendations on the need to further subdivide the EKC into HLRs. Results for both regional curve and hydraulic geometry curve analyses suggest that datasets from the EKC may be supplemented using data from other physiographic regions in the U.S. as long as the data are obtained from the same HLR.

References

Agouridis, C.T., R.A. Brockman, S.R. Workman, L. Ormsbee, and A.W. Fogle. 2011. Bankfull hydraulic geometry relationships for the Bluegrass Region of Kentucky. Water 3: 923-948.

Blackburn-Lynch, W. 2015. Development of techniques for assessing and restoring streams on surface mined lands. Ph.D. dissertation, University of Kentucky.

Brockman, R.A., C.T. Agouridis, S.R. Workman, L.E. Ormsbee, and A.W. Fogle. 2012. Bankfull regional curves for the Inner and Outer Bluegrass regions of Kentucky. *Journal of the American Water Resources Association* 48: 391-406.

Harrelson, C.C., Rawlins, C., Potyondy, J., 1994. Stream Channel Reference Sites: An Illustrated Guide to Field Techniques. USDA Forest Service Rocky Mountain Forest adn Range Experiment Station General Technical Report RM245, 67.

Hession W.C., J.E. Pizzuto, T.E. Johnson, and R.J. Horwitz. 2003. Influence of bank vegetation on channel morphology in rural and urban watersheds. Geology 31: 147-150.

Wolock, D.M., T.C. Winter, and G. McMahon. 2004. Delineation and evaluation of hydrologic-landscape regions in the United States using geographic information system tools and multivariate statistical analyses. Environmental Management 34: S71-S88.

[USGS] U.S. Geological Survey. 1982. Bulletin 17B, Guidelines for determining flood-flow frequency. Hydrology Subcommittee of the Interagency Advisory Committee on Water Data, Reston, VA.

The use of eDNA to detect bacterial genetic markers associated with fecal contamination in the Triplett Creek Watershed, Rowan County, Kentucky

Basic Information

Title:	The use of eDNA to detect bacterial genetic markers associated with fecal contamination in the Triplett Creek Watershed, Rowan County, Kentucky
Project Number:	2016KY260B
Start Date:	3/1/2016
End Date:	2/28/2018
Funding Source:	104B
Congressional District:	KY 5th
Research Category:	Water Quality
Focus Category:	Management and Planning, Water Quality, Wastewater
Descriptors:	None
Principal Investigators:	Geoff Gearner

Publication

1. Brown, Rachel, Hannah Conley and Geoffrey Gearner, 2017, The Use of Environmental DNA to Detect Bacterial Molecular Markers in the Triplett Creek Watershed, Rowan County, Kentucky, in Proceedings of the 2017 Kentucky Water Resources Annual Symposium, Kentucky Water Resources Research Institute, Lexington, Kentucky, p. 77.

The Use of eDNA to Detect Bacterial Genetic Markers Associated with Fecal Contamination in the Triplett Creek Watershed, Rowan County, Kentucky

Problem and Research Objectives

The objective of the study was to develop and evaluate the use of bacterial genetic targets as markers of fecal contamination in the Triplett Creek Watershed for the purpose of identifying point and host sources of fecal pollution. Specifically, this project is using quantitative polymerase chain reaction (qPCR) to evaluate DNA extracted from filtered water samples (commonly referred to as environmental or eDNA) collected from long standing sampling sites in the Triplett Creek Watershed for the presence of genetic markers associated with fecal bacteria. Collected data could then be used to construct plume maps of human and/or cattle fecal-associated bacteria. The fieldwork started in May 2016, with the lab work beginning shortly thereafter, and continuing through November 2016. Our objective remains unchanged, although the project is being extended into the early part of 2017 to obtain additional data.

Methodology

The one change we have made in our methodology is in the way we collect samples. We originally proposed using a peristaltic pump to filter water samples in the field at our sampling sites in the Triplett Creek Watershed. In consulting with others who work with eDNA, we decided to collect 3-liter samples in sample collection bottles, then transport the samples to the microbiology lab for filtration. There are a number of advantages, including reducing the risk of sample contamination. The other advantage is cost savings for the project.

Findings and Significance.

With wet weather returning to Northeast Kentucky in late Fall/early Winter, we were able to collect water from 12 sampling sites in the Triplett Creek Watershed. Extraction of eDNA from the glass fiber filters (Qiagen protocol) and clean-up (Zymo Research protocol) provided eDNA yields of 3-83 ng/µL. Initial endpoint PCR analysis of eDNA samples detected the bacterial 16S ribosomal gene, *E. coli* (*uidA* gene), and the antibiotic resistance genes *ereA* (erythromycin resistance) and *bla*^{TEM}

(an extended spectrum beta-lactamase gene). We are encouraged by these early results, which suggests that eDNA can be used to detect bacterial pollutants in surface waters.

Since our original proposal was submitted, we have decided on these modifications to the project: 1) Addition of an exogenous internal positive control to all endpoint PCR reactions, and 2) Using Taqman Environmental Master Mix (designed for PCR of eDNA). PCR target genes we are evaluating via endpoint PCR:

Primer Name	Primer Sequence	Target
TetW-F	5'-GAGAGCCTGCTATATGCCAG-3'	tetracycline resistance gene
TetW-R	5'-GGGCGTATCCACAATGTTAAC-3'	
TetO-F	5'-ACGGARAGTTTATTGTATACC-3'	tetracycline resistance gene
TetO-R	5'-TGGCGTATCTATAATGTTGAC-3'	
SulI-F	5'-CGCACCGGAAACATCGCTGCAC-3'	sulfonamide resistance gene
SulI-R	5'-TGAAGTTCCGCCGCAAGGCTCG-3'	
SulII-F	5'-TCCGGTGGAGGCCGGTATCTGG-3'	sulfonamide resistance gene
SulII-R	5'-CGGGAATGCCATCTGCCTTGAG-3'	
ereA-F	5'-ATGACGTGGAGAACGACCAG-3'	erythromycin resistance gene
ereA-R	5'-CCGACAATTCGGGCGCCCTCAAT-3'	
msrA/B-F	5'-CTGGAACGGTTGAAACGGATGGC-3'	macrolide resistance gene
msrA/B-R	5'-ACCACCACTCATACTGTCGGTTG-3'	
HF183F	5'-ATCATGATGTCACATGTCCG-3'	human-specific bacterial marker
CF128F	5'-CCAACYTTCCCGWTACTC-3'	cattle-specific bacterial marker
Bac708R	5'-CAATCGGAGTTCTTCGTG-3'	
espF	5'-TATGAAAGCAACAGCACAAGTT-3'	human bacterial marker
espR	5'-ACGTCGAAAGTTCGATTTCC -3'	
bla-TEM-F	5'-GCGGAACCCCTATTTG-3'	ESBL gene
bla-TEM-R	5'-ACCAATGCTTAATCAGTGAG-3'	
bla-SHV-F	5'-TTATCTCCCTGTTAGCCACC-3'	ESBL gene
bla-SHV-R	5'-GATTTGCTGATTTCGCTCGG-3'	
bla-CMY-F	5'-ATGATGAAAAAATCGTTATGCT-3'	ESBL gene
bla-CMY-R	5'-TTATTGCAGCTTTTCAAGAATGCG-3'	

All supplies for this work have been purchased. Positive PCR results will be confirmed by DNA sequencing of PCR products (GeneWiz). We will follow up positive PCR results with quantitative/real time PCR. This additional work will be supported in part by Kentucky Biomedical Research Infrastructure Network funding. A side project has also emerged. We have purchased PCR primers for the detection of *Giardia intestinalis* and *Cryptosporidium parvum*, along with positive controls for these water-borne parasitic protozoans (these additional materials were purchased with Morehead State University Biology and Chemistry departmental funds). A no-cost extension has been granted for this project. Low flows during summer 2016 limited opportunities for sampling. As a result, plans are now to continue sampling and analysis through the wetter spring months of 2017 in order to gather more data for evaluation.

Climate change impacts on soil-water availability under different land management: forest and grasslands

Basic Information

Title:	Climate change impacts on soil-water availability under different land management: forest and grasslands
Project Number:	2016KY261B
Start Date:	3/1/2016
End Date:	2/28/2018
Funding Source:	104B
Congressional District:	KY 1st & 2nd
Research Category:	Climate and Hydrologic Processes
Focus Category:	Agriculture, Conservation, Geochemical Processes
Descriptors:	None
Principal Investigators:	Brad Lee

Publications

1. Baker, Trinity J., T.N. Williamson, and Brad Lee, 2016, Comparing Simulated Soil Properties to Field Derived Values in Forested and Grassland Catenas of MLRA 120, in Proceedings of the 2016 Kentucky Water Resources Annual Symposium, Kentucky Water Resources Research Institute, Lexington, Kentucky, p. 29.
2. Williamson, Tanja N., Brad D. Lee, and Trinity J. Baker, 2017, Projections of 2050 Soil-Water Storage Under Differing Land Management, in Proceedings of the 2017 Kentucky Water Resources Symposium, Kentucky Water Resources Research Institute, Lexington, Kentucky, p. 53.
3. Baker, Trinity, 2017, MS Thesis, Soil Hydraulic Property Estimation Under Major Landuses in the Shawnee Hills, Department of Plant and Soil Science, College of Agriculture Food and Environment, University of Kentucky, Lexington, Kentucky, 371 p. http://uknowledge.uky.edu/pss_etds/86

Climate Change Impacts on Soil-Water Availability Under Different Land Management: Forest and Grasslands

Problem and Research Objectives

In recent years, the USDA NRCS has emphasized and incentivized the introduction of cover crops and crop rotations into agricultural systems in order to increase soil organic carbon (OC) stocks and thus improve soil quality resulting in agronomic benefits (e.g. increased yields due to higher nutrient retention, improved soil health, and increased soil biota diversity). However these results have not been demonstrated in a research environment but rather are supported by anecdotal evidence from a few early adopters in northern climates where soil OC contents are naturally much higher than in Kentucky soils. Further interest in improving OC contents in soils is partially due to the potential improvements to soil hydraulic properties including plant- available water-holding capacity and infiltration. This in-turn results in better agronomic resiliency under drought conditions. Soil OC content has been linked to available water-holding capacity and saturated hydraulic conductivity (Ksat), however these hydrologic soil properties are also dependent on other soil factors, including particle-size distribution and bulk density (Saxton and Rawls, 2006; Rawls et al. 1983, 2003).

The objectives of this study are to: 1) Develop a better understanding of the effect of soil OC, as it varies with land cover, on soil-water holding capacity; 2) Demonstrate how the RaCA soil samples that were collected as part of the 2010-2013 national study can complement local field studies; 3) Illustrate how land management can enable agricultural resilience; and 4) Provide a means of discussing agricultural resilience as a function of land management with the agricultural community.

Methodology

In order to provide those hydrologic soil-property data necessary to simulate soil-water storage, we estimate saturated hydraulic conductivity (Ksat), total porosity, 33 kPa (field capacity - FC) water retention, and plant available water holding capacity (AWC) using a series of equations that incorporate total sand, silt, clay and organic carbon abundance in individual horizons (Saxton and Rawls, 2006). This method provides a consistent approach to estimating hydrologic soil properties with a minimum of soil physical data. We will also use these equations for soil material sampled from the Shawnee Hills forest and grassland sites in order to demonstrate how this approach compares to field and lab characterization of soil from local field description. This same approach will then be used to incorporate the samples from the national Rapid Assessment of U.S. Soil Carbon (RaCA) which provides a recent snapshot of OC storage across the country and under different land covers.

We compare soil-hydrologic properties estimated using established equations (Saxton and Rawls, 2006) to those quantified by field and laboratory procedures for soils from the Shawnee Hills Loess Catenas Soil Systems project in MLRA 120. These sites have been used in previous research on modeling soil-water storage (Williamson et al., 2014). We apply the same equations and hydrologic modeling to RaCA samples and data collected within MLRA 120 (including those from forest, pasture, traditional agriculture, and Conservation Reserve Program [CRP] lands) with the objective of simulating soil-water availability with forecasted climate under different land management. This work utilizes soils information collected from 2 studies: The Shawnee Hills Project and the USDA NRCS RaCA program.

The Shawnee Hills Project was the first "Soil Systems" approach for the USDA NRCS Soil Survey (Schoeneberger et al, 2013). This soil systems approach utilizes these sites as a framework for understanding and communicating soil processes, collecting geographic soil information, and designing soil investigations. Specifically, the Shawnee Hills project involves 3-paired catchments (total of 6) under grass and forest land use that are representative of the major soils in the MLRA 120, an approximately 3.5 million ha (8.65 million acres) area in western Kentucky, southern Indiana, and southern Illinois (Figure 1). Within each catchment, benchmark catenas (toposequences) with different loess thicknesses were sampled, described, and characterized according to standard USDA NRCS procedures (Schoeneberger et al., 2002 and Soil Survey Staff, 2009).

The USDA RaCA program was initiated in 2010 to assess the soil organic carbon stocks in the United States. Soil samples were collected and analyzed for their organic carbon (OC) content by soil horizon to a depth of 100 cm at 6417 randomly selected Natural Resource Inventory long-term land use-land cover monitoring points across the nation. At each site, a central pedon was described in detail and sampled together with four satellite locations at 30-m distance along the four cardinal directions. This sampling strategy provides an understanding of variability that is analogous to what is provided by the five landscape positions sampled for the Shawnee Hills sites.

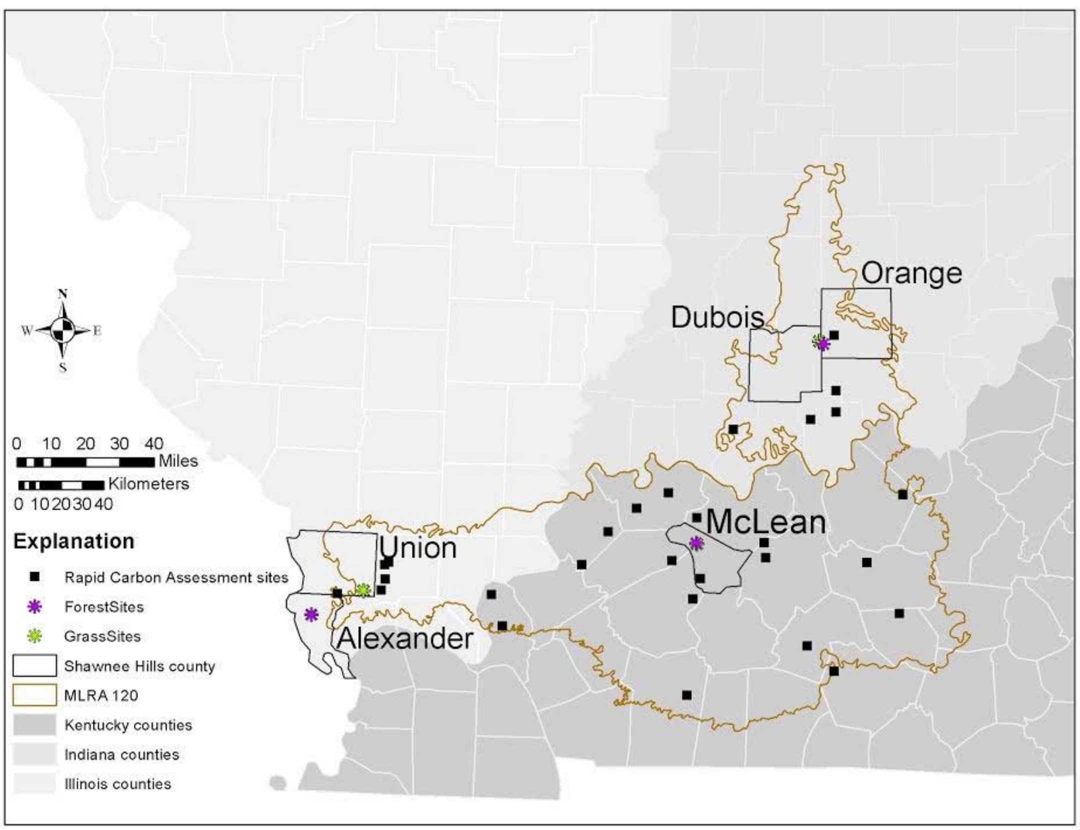

Fig. 1. Location of MLRA 120, RaCA and Shawnee Hills project catchments relative to western Kentucky.

The Shawnee Hills catchments were delineated based on landscape position (summit, shoulder, backslope, footslope, and toeslope). At least one representative pedon within each landscape position was described and sampled in a soil pit according to standard USDA NRCS Soil Survey methods (Schoeneberger et al., 2002). Horizons were sampled and the less than 2 mm fraction was characterized for OC (combustion method used as no carbonate minerals or coal-rich layers were present – Soil Survey Staff, 2009), particle size and textural class (Gee and Bauder, 1986). Saturated hydraulic conductivity was determined at 3 to 4 depths using a 10-cm head height (Amoozegar, 1989) and 5 replicates within 5 m of the pedon sample location.

The RaCA project characterized soils in 6417 sites across the nation for the purpose of collecting a soil OC inventory under representative land use-land cover classifications. Each site included a central pedon and 4 satellite pedons described and sampled by horizon to a depth of 100 cm for bulk-density, particle size analysis and soil OC analysis (USDA NRCS, 2016). Twenty-eight RaCA sites were selected for this proposed work based on location (within MLRA 120A & 120B) and parent material (loess over residuum to match the Shawnee Hills project pedons). The land use-land cover within these selected sites includes cropland, forest, grassland and CRP.

Using equations from Saxton and Rawls (2006), we estimate the hydrologic properties of soils under different land covers. These estimates will be evaluated using the well-characterized pedons in the Shawnee Hills project. Then the RaCA sites from MLRA 120, representing agriculturally important soils in western Kentucky, will be used to estimate the amount of plant available water under historical climate and forecasted climate. Each of these analyses will use a previously calibrated and statistically evaluated hydrologic model for a 0.05 km^2 basin (Williamson et al., 2014). Plant available water will be compared as seasonal averages over a 25-yr time period (1990-2014 and 2037-2062) to quantify the ability to continue agricultural production when different covers are incorporated as part of land management.

Principal Findings and Significance

This research takes advantage of the RaCA dataset as well as ongoing work in the Shawnee Hills project and is a demonstration of how this national inventory of carbon storage can be incorporated into a better understanding of agricultural resiliency, soil-water storage, and, ultimately, response of the landscape to drought conditions and the shift in seasons that are forecasted for this area of the U.S.

Estimates of plant available soil water holding capacity and hydraulic conductivity have been developed using pedotransfer functions for loess covered RaCA sites in Shawnee Hills. These pedotransfer functions were developed using six well-characterized forested and grassed catenas in western Kentucky, southern Indiana, and southern Illinois and then verified on two additional well-characterized catenas in the Shawnee hills. The USGS IN-KY Water Sciences Center is completing their contribution to the project and we anticipate the climate model results in May 2017. The project has been granted a one-year no-cost extension to complete the overall effort. Remaining tasks include development of a publication for the Soil Science Society of America Journal (anticipated submission December 2017) and a bulletin for Cooperative Extension Service Agriculture and Natural Resources agents (anticipated submission to University of Kentucky Agricultural Communications Services December 2017).

References

Amoozegar, A. 1989. A compact constant-head permeameter for measuring saturated hydraulic conductivity of the vadose zone. *Soil Sci. Soc. Am. J.* 53:1356-1361.

Gee, G.W., and J.W. Bauder. 1986. Particle-size analysis. p. 383-411. *In* A. Klute (ed.) Methods of soil analysis. Part 2. 2nd ed. Agron. Monogr. 9 ASA and SSSA, Madison, WI.

Rawls, W.J. and D.L. Brakensiek. 1983. A procedure to predict Green and Ampt. Infiltration parameters, Advances in infiltration. Proc. Of the Nat'l Conference on Advances in Infiltration, Chicago, IL.

Rawls, W.J. Y.A. Pachepsky, J.C. Ritchie, T.M. Sobecki, H. Bloodworth. 2003. Effect of soil organic carbon on soil water retention. *Geoderma* 116: 61-76.

Saxton K.E., Rawls W.J. 2006. Soil Water Characteristic Estimates by Texture and Organic Matter for Hydrologic Solutions. *Soil Science Society of America Journal* 70:1569-1578. DOI: 10.2136/sssaj2005.0117.

Schoeneberger, P.J., Wysocki, D.A., Benham, E.C., and Broderson, W.D. (editors), 2002. Field book for describing and sampling soils. Version 2.0. NRCS, National Soil Survey Center, Lincoln, NE.

Schoeneberger, P.J. Z. Libohova, D.A. Wysocki, B.D. Lee and S.J. Indorante. 2013. Soil landscape systems as a framework for understanding and communicating soil processes, geographic soil information and for designing soil investigations. Soil Science Society of America Annual Meeting, Tampa. FL.

Soil Survey Staff. 2009. Soil survey field and laboratory methods manual. Soil Survey Investigations Report No. 51, Version 1.0. R. Burt (ed.). USDA, NRCS.

United States Department of Agriculture, Natural Resources Conservation Service, 2016. Rapid Carbon Assessment (RaCA): Methodology, Sampling, and Summary, USDA, NRCS, 24 p.

Williamson, T.N., B.D. Lee, P.J. Schoeneberger, W.M. McCauley, and S.J. Indorante. 2014. Simulating soil-water movement through loess veneered landscapes using non-consilient soil properties. *Soil Sci. Soc. Am. J.* doi: 10.2136/sssaj2014.01.0045

Impact of climate change on extreme hydrologic events in the Kentucky River Basin

Basic Information

Title:	Impact of climate change on extreme hydrologic events in the Kentucky River Basin
Project Number:	2016KY262B
Start Date:	3/1/2016
End Date:	2/28/2017
Funding Source:	104B
Congressional District:	KY 5th & 6th
Research Category:	Climate and Hydrologic Processes
Focus Category:	Climatological Processes, Drought, Floods
Descriptors:	None
Principal Investigators:	Dwayne R. Edwards

Publication

1. Chattopadhyay, S. and Dwayne Edwards, 2017, Assessing Climate Change Impacts on Future Water Availability and Droughts in the Kentucky River Basin, in Proceedings of the 2017 Kentucky Water Resources Annual Symposium, Kentucky Water Resources Research Institute, Lexington, KY, p. 27.

Assessing Climate Change Impacts on Future Water Availability and Droughts in the Kentucky River Basin

Problem and Research Objectives

The current century is an era of ubiquitous climate change (Green et al., 2011) and studies having a variety of provenances agree on the major role of anthropogenic global warming (Haddeland et al., 2014). Vijayavenkatraman et al. (2012) pointed out that there has always been variation in the earth's climate, but the recent and rapid changes on a global scale are of growing concern. In the U.S., for example, Diffenbaugh and Ashfaq (2010) have reported that exceptionally long heat waves and other hot events could become commonplace in the next 30 years (2010-2039). Higher future temperatures can increase rates of hydrologic system losses to evaporation and transpiration and, in turn, produce more rainfall. As a result, the Intergovernmental Panel on Climate Change (IPCC) has noted a widespread sense among climate scientists that extreme events (e.g., droughts and floods) will become increasingly frequent, intense and widespread in the future (IPCC, 2007).

The objective of this study was to evaluate the potential impacts of climate change on droughts in the Kentucky River basin in the southeastern US (Figure 1). The focus was on meteorological and hydrological droughts, since agricultural production within the basin is relatively low. The findings can inform policy makers and resources managers on beneficial courses of action to ensure sustained water availability during changing climate.

Methodology

This study evaluated the potential impacts of climate change on hydrologic processes in the Kentucky River basin using the Soil and Water Assessment Tool (SWAT). The SWAT model was selected for use due to its widespread use and the compatibility between previously reported SWAT model applications and the objectives of this study. The SWAT model was calibrated and validated for three gaging stations in the watershed: Lockport (station 03290500), Frankfort (station 03287500) and Booneville (station 03281500).

Bias corrected (Multivariate Adopted Constructed Analogue or MACA; Abatzoglou and Brown, 2012) 4-km resolution daily data on precipitation and maximum and minimum temperature were obtained from the University of Idaho (http://maca.northwestknowledge.net/index.php) for 10 global climate models (GCM). The MACA algorithm is a statistical downscaling method, capable of transferring GCM outputs to the spatial scales necessary for impact modelling while preserving meteorological patterns and spatiotemporal properties of the data. The GCM data reflect two representative concentration pathway (RCP) scenarios, RCP 4.5 and RCP 8.5, which are indicative of medium and high emission of carbon respectively. Data were obtained for the periods 1976 – 2005 (defined as the *baseline period*), 2036 – 2065 (the *mid-century period*) and 2070-2099 (the *late-century period*).

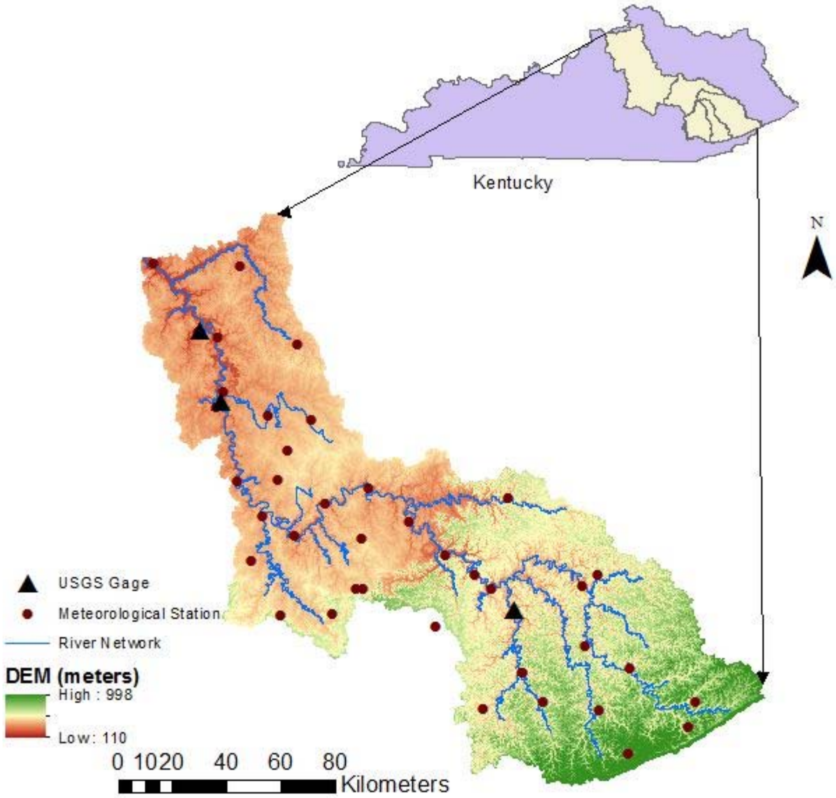

Figure 1. Location of the Kentucky River Basin in north-central Kentucky showing the USGS streamflow gages and weather stations

Two basic indices were used in defining drought events and in assessing their intensity: the reconnaissance drought index (RDI) and streamflow drought index (SDI). The RDI is a relatively recently-developed meteorological index that accounts for both precipitation and potential evapotranspiration in calculating water deficits (Tsakiris et al. 2007). The gamma probability density function was used to model the distribution of α_k, and monthly values of standardized RDI were computed in this study. Positive and negative values of RDI indicate wet and dry periods, respectively, while more negative values represent more severe droughts. The SDI (Hong et al. 2015) is a hydrological drought index that is calculated on the basis of cumulative streamflow volumes $S_{i,k}$ for each reference period *k* of the *i*-th hydrological year. Monthly streamflow data from the SWAT model simulation were fitted using the gamma distribution function to calculate monthly SDI values. As with the RDI, positive values of SDI reflect relatively wet conditions, while negative values indicate hydrological drought.

A *drought event* was defined as a duration over which both the RDI and SDI were continuously negative. Drought onset was therefore determined as the month in which both RDI and SDI values first became negative, while the drought was considered as ending on the first month for which either RDI or SDI became positive. Additional indices were calculated to indicate drought magnitude for each identified drought event.

For a drought event of duration n months, drought severity (S) was calculated as the sum of absolute RDI/SDI values over that duration. Since S was calculated on the basis of both RDI and SDI values,

$$S_{RDI} = \sum_{j=1}^{n} |RDI_j| \quad (1)$$

and

$$S_{SDI} = \sum_{j=1}^{n} |SDI_j| \quad (2)$$

Drought intensity (I) was calculated as mean S over the drought event:

$$I_{RDI} = \frac{S_{RDI}}{n} \quad (3)$$

$$I_{SDI} = \frac{S_{SDI}}{n} \quad (4)$$

Maximum Drought Length (MDL) was calculated as the maximum drought event over each of the three timeframes investigated (historical, mid-century and late-century) for each of the subwatersheds.

Principal Findings and Significance

<u>Climate Change Impact Analysis</u>

Evapotranspiration

The spatial distribution of projected changes in ET is shown in Fig. 2. As indicated, all of the 49 subwatersheds are projected as having ET increases in both the mid- and late-century periods, with spatial similarities between the RCPs in terms of relative magnitudes of increase. The timeframes and RCPs are consistent in projecting the north-central portion of the basin as having the largest increases in ET. Coincidentally, this portion of the basin is in proximity to the Lexington-Fayette metropolitan statistical area, which has a population of nearly 500,000.

Water Yield

The spatial distribution of projected water yield changes is shown in Fig. 3. For mid-century projections, all but one of the 49 subwatersheds are projected to experience water yield increases. Late-century projections for RCP 8.5 indicate the same result (and involving the same subwatershed), while RCP 4.5 projections identify approximately 88% of the subwatersheds as experiencing water yield increases. The portion of the basin having decreasing projected water yields (north-central) is also associated with the highest projected ET values (Fig. 2), suggesting the importance of ET in the context of water yield for this region.

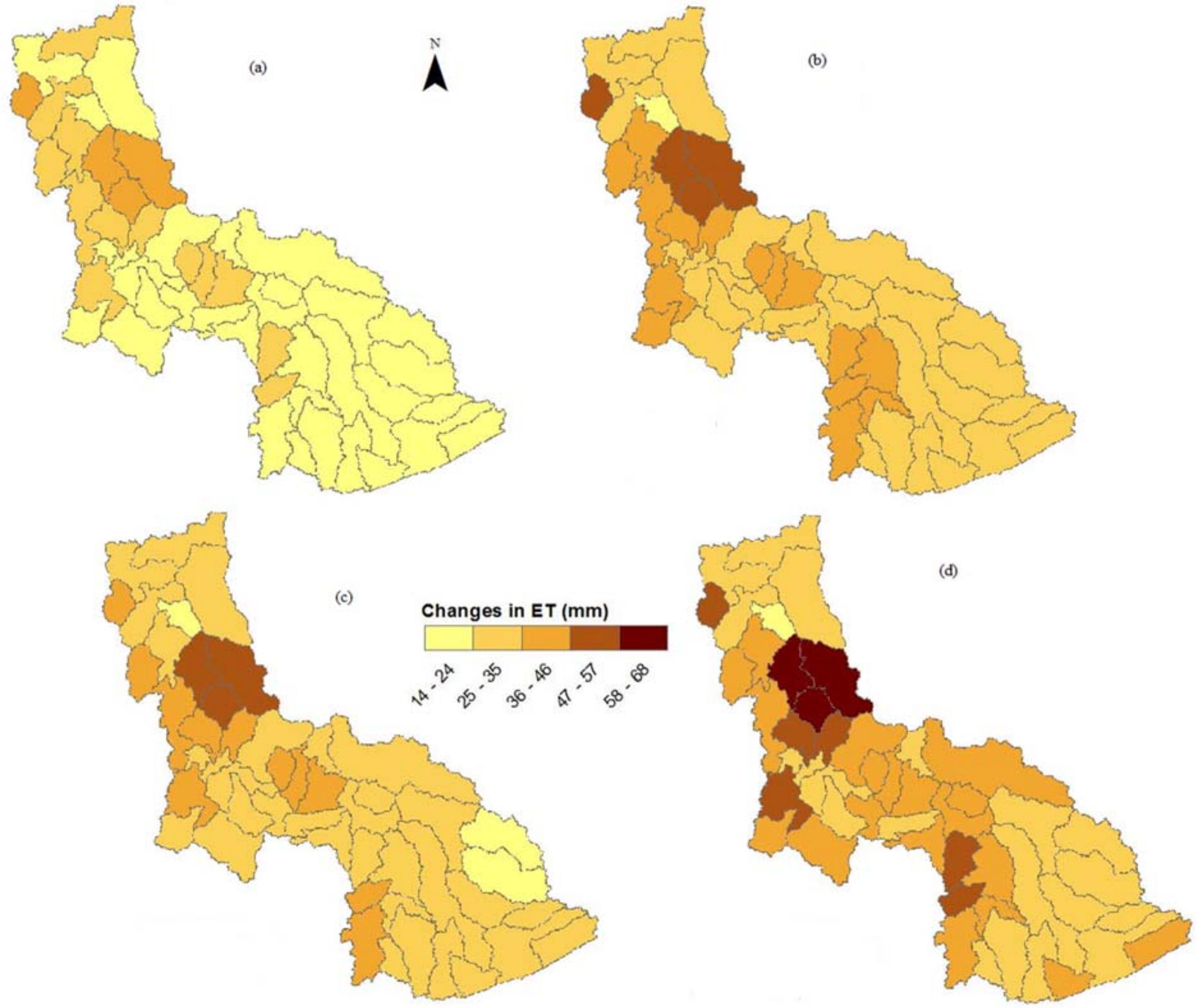

Figure 2. Change in mean annual ET (from baseline) (a-b) in the mid -century and late-century (c-d) under RCP 4.5 and RCP 8.5 respectively.

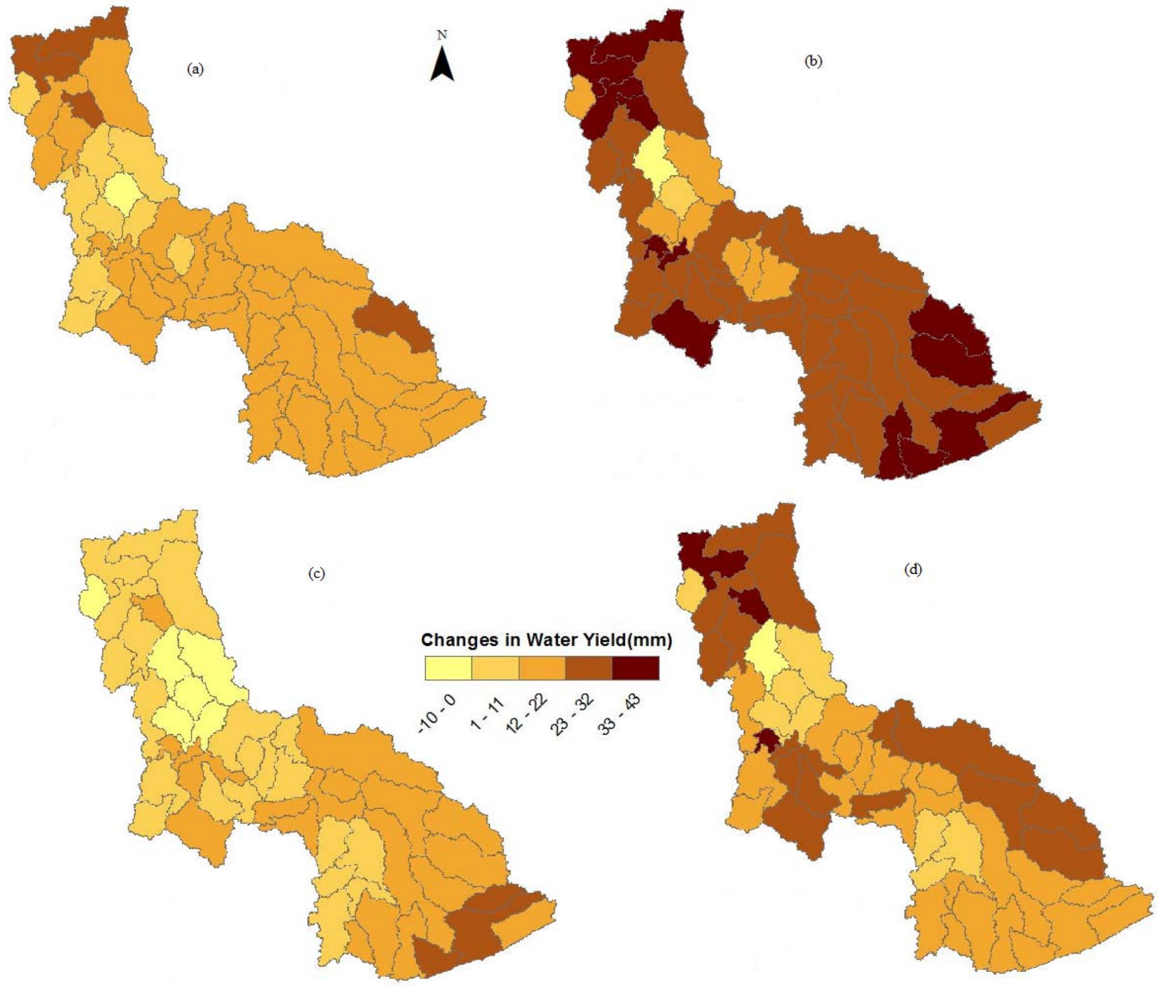

Figure 3. Change in mean annual water yield (from baseline) (a-b) in the mid -century and late-century (c-d) under RCP 4.5 and RCP 8.5 respectively

Drought Analysis

Overview

Analysis of RDI drought durations for each of the 49 subwatersheds indicated average drought lengths of 1-4 months, with 80% in the 3-4 month range (Fig. 4(a)) for the baseline period. Projected average drought durations were similar for the mid-century timeframe but exhibited more differences for the late-century. The late-century RCP 4.5 scenario indicated subwatersheds shifting from the 1-2 month into the 3-4 month average drought duration category, while the reverse was true for RCP 8.5. In comparison to the RDI findings, Fig. 4(b) indicates that droughts as defined the SDI are of a more chronic nature; for the baseline timeframe, roughly 45% of subwatersheds had average drought lengths of 4-5 months. Projected average drought (SDI) lengths were consistent for all timeframes and RCP scenarios except for late-century RCP 8.5 which, similar to RDI-defined drought lengths, demonstrated a shift of subwatersheds away from the 4-5 month and toward the 3-4 month average drought length category.

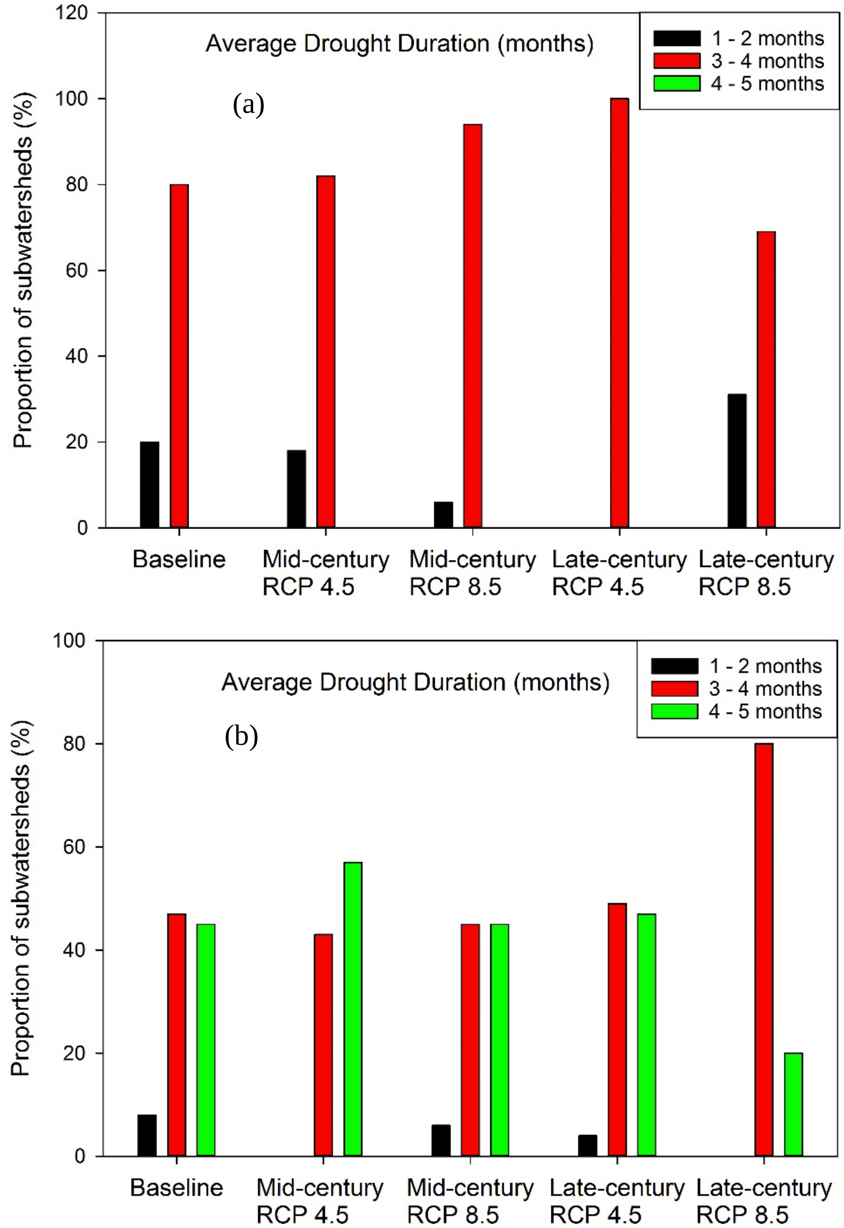

Figure 4. Proportion of subwatersheds in average drought length categories as defined by (a) RDI and (b) SDI.

Maximum Drought Length

Basin-wide Maximum Drought Lengths (MDLs) are given in Table 1 for all timeframes/scenarios and for both RDI- and SDI-defined droughts. Consistent with previous discussion, Table 1 reflects the more persistent nature of hydrological droughts (SDI) relative to meteorological droughts (RDI), with MDLs for SDI-defined droughts being about 50% greater than those for RDI-defined droughts. Projected MDL deviations from the baseline timeframe tended to be relatively small except for the mid-century RCP 4.5 projections, which were associated with a 25% increase in SDI-defined MDL.

Table 1 Basin-wide duration and intensity of drought events calculated from RDI/SDI values for the Kentucky River Basin

Scenario	Maximum Drought Length		Average Drought Intensity	
	RDI	SDI	RDI	SDI
	----- Months -----			
Baseline	8	12	1.38	1.20
Mid-century				
RCP 4.5	9	15	1.37	1.11
RCP 8.5	7	13	1.31	1.24
Late-century				
RCP 4.5	8	12	1.33	1.17
RCP 8.5	9	13	1.27	1.14

The spatial distribution of MDL for the baseline timeframe is shown in Figure 5, which indicates that the southern portion of the basin experienced greater MDLs for both RDI- and SDI-defined droughts. Figure 5(b) also indicates that the region of greatest MDL is coincident with the previously-discussed Lexington-Fayette area, the most heavily developed region in the basin.

Differences in spatial MDL distribution due to type of drought and RCP scenario are apparent in Fig. 6 for projected mid-century MDL values. The RCP 4.5 projections indicate that the northern portion of the basin is generally associated with increasing MDL for both RDI- and SDI-defined droughts. In contrast, RCP 8.5 projections indicate near-uniform decreases in MDL for meteorological drought, with increasing MDL for hydrological drought associated primarily with the southern basin. More consistency is apparent in late-century MDL projections, as shown in Fig 7. For both RDI- and SDI-defined droughts, the highest MDL values are generally, though with some variation, associated with the northern and central portions of the basin.

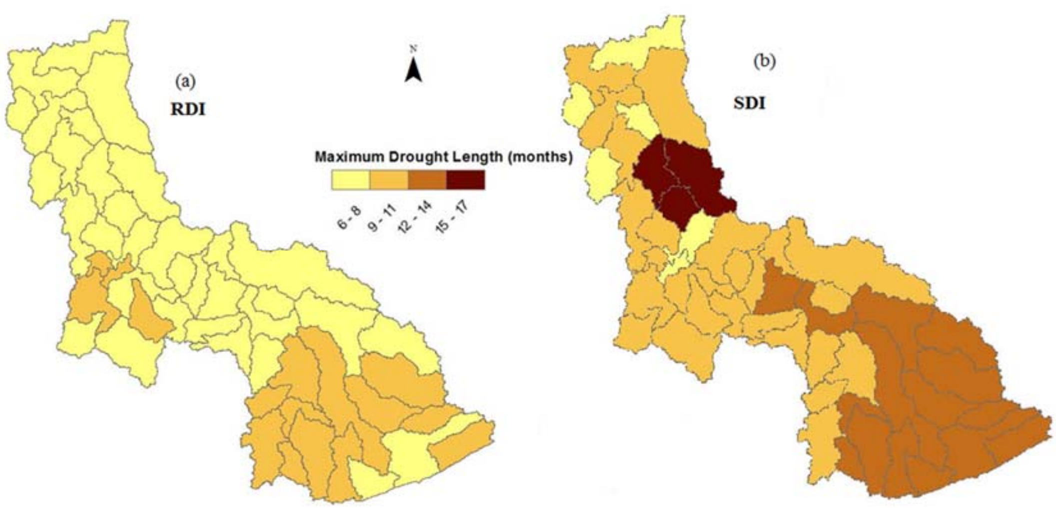

Figure 5. Spatial distribution of maximum drought length calculated from a) RDI and b) SDI values in the baseline

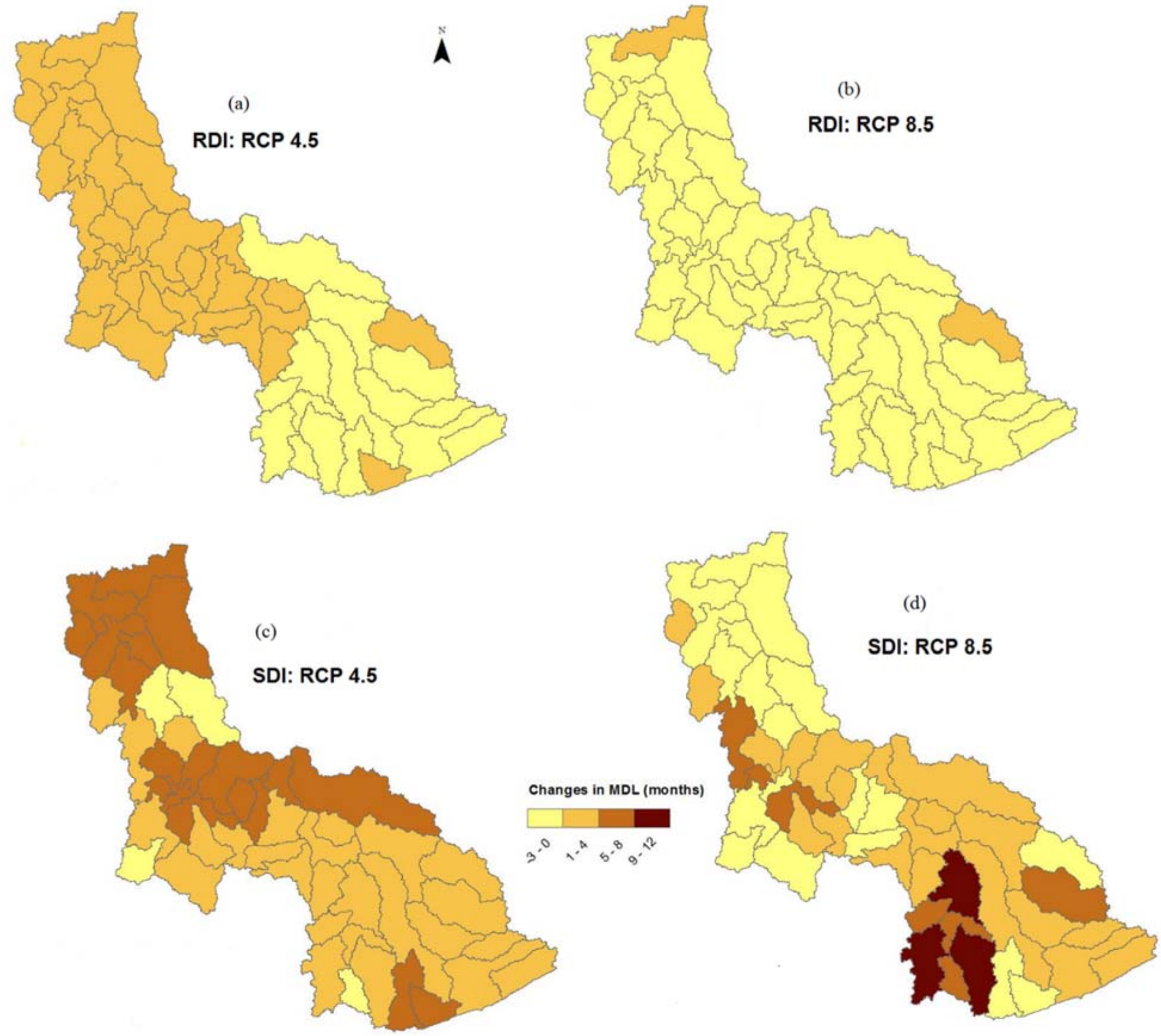

Figure 6. Spatial distribution of changes in maximum drought length in the mid-century calculated from RDI (a-b) and SDI (c-d) under RCP 4.5 and 8.5 respectively

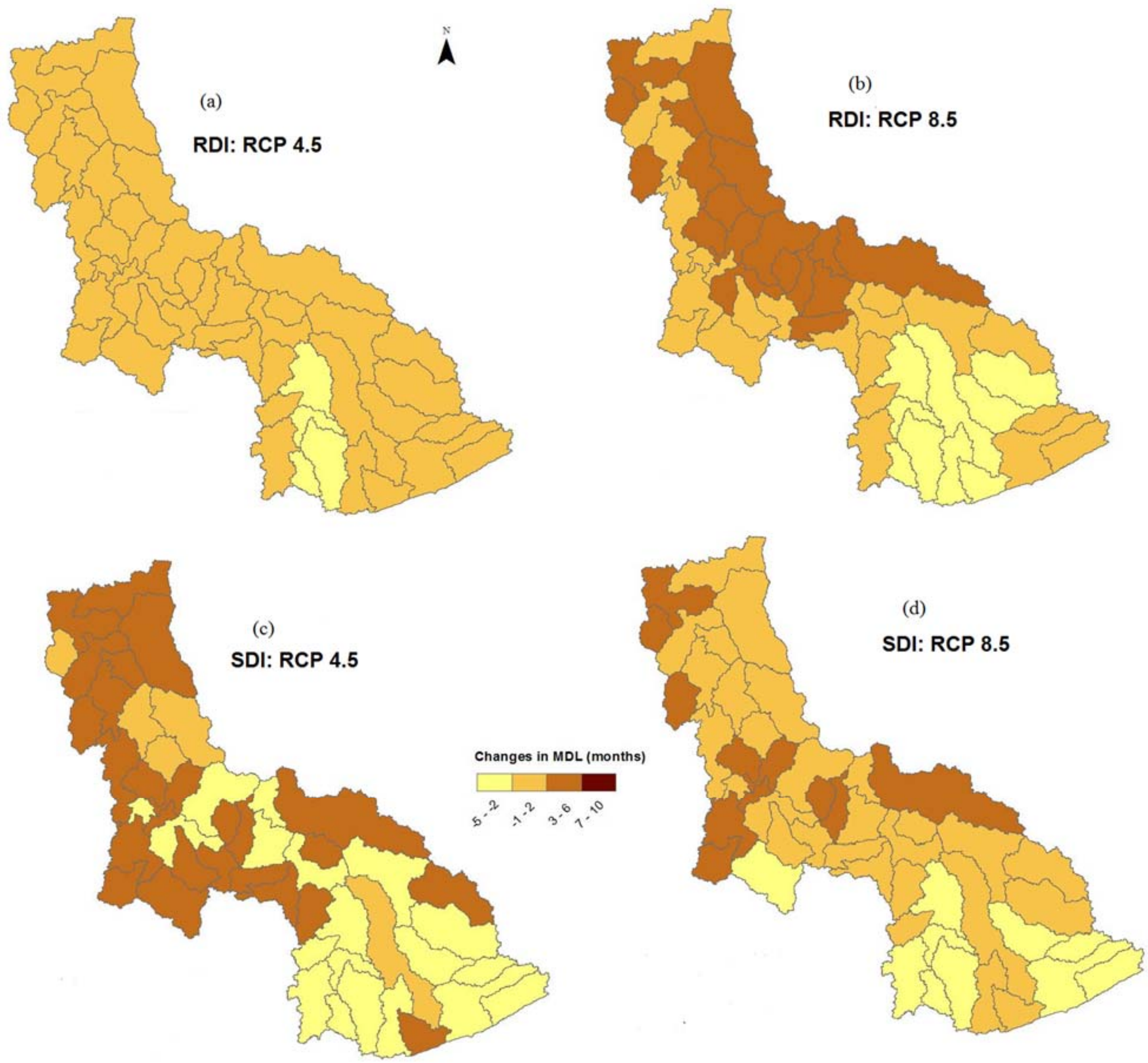

Figure 7. Spatial distribution of changes in maximum drought length in the late-century calculated from RDI (a-b) and SDI (c-d) under RCP 4.5 and 8.5 respectively

Drought Intensity

In contrast to the findings for MDL, basin-wide average intensities were lower for SDI-defined droughts (1.20) than for RDI-defined droughts (1.38) during the baseline period (Table 1). This result suggests that hydrologic droughts, insofar as regards their intensity, experienced a damping effect, perhaps as a result of the additional processes and storages involved. The same relationship was generally (with the exception of mid-century, RCP 8.5) true for drought projections for all timeframes and scenarios. Additionally, with the same exception, intensities of both SDI- and RDI-defined basin-wide droughts decreased relative to the baseline period for all drought projections.

The spatial distribution of projected drought intensities (Figs. 8 and 9) is quite complex. Mid-century drought intensity projections (Fig. 8) demonstrate no clear pattern of behavior with the possible exception of a tendency toward more intense droughts (as defined by both indices) in the northern and eastern portions of the basin, with subwatersheds projected as having less intense droughts scattered throughout. Late-century drought projections (Fig. 9) are similarly complex in terms of spatial distribution, but possibly more RCP-dependent than mid-century projections. Projections for RCP 4.5 suggest that the highest increases in drought (both meteorological and hydrological) intensity are associated with the northern portion of the basin, whereas these increases are associated more with the southern portion for RCP 8.5.

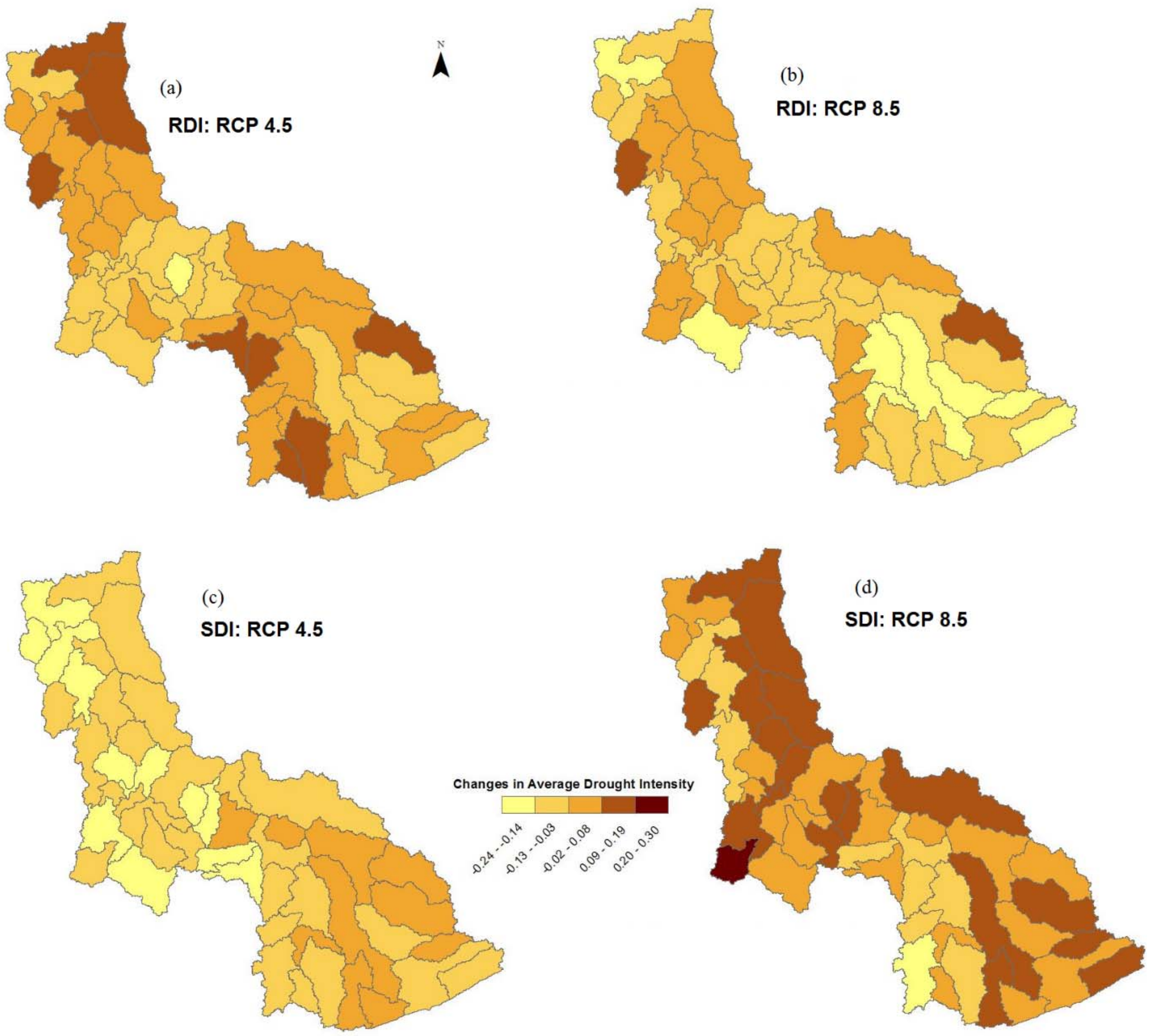

Figure 8. Spatial distribution of changes in drought intensity in the mid-century calculated from RDI (a-b) and SDI (c-d) under RCP 4.5 and 8.5 respectively

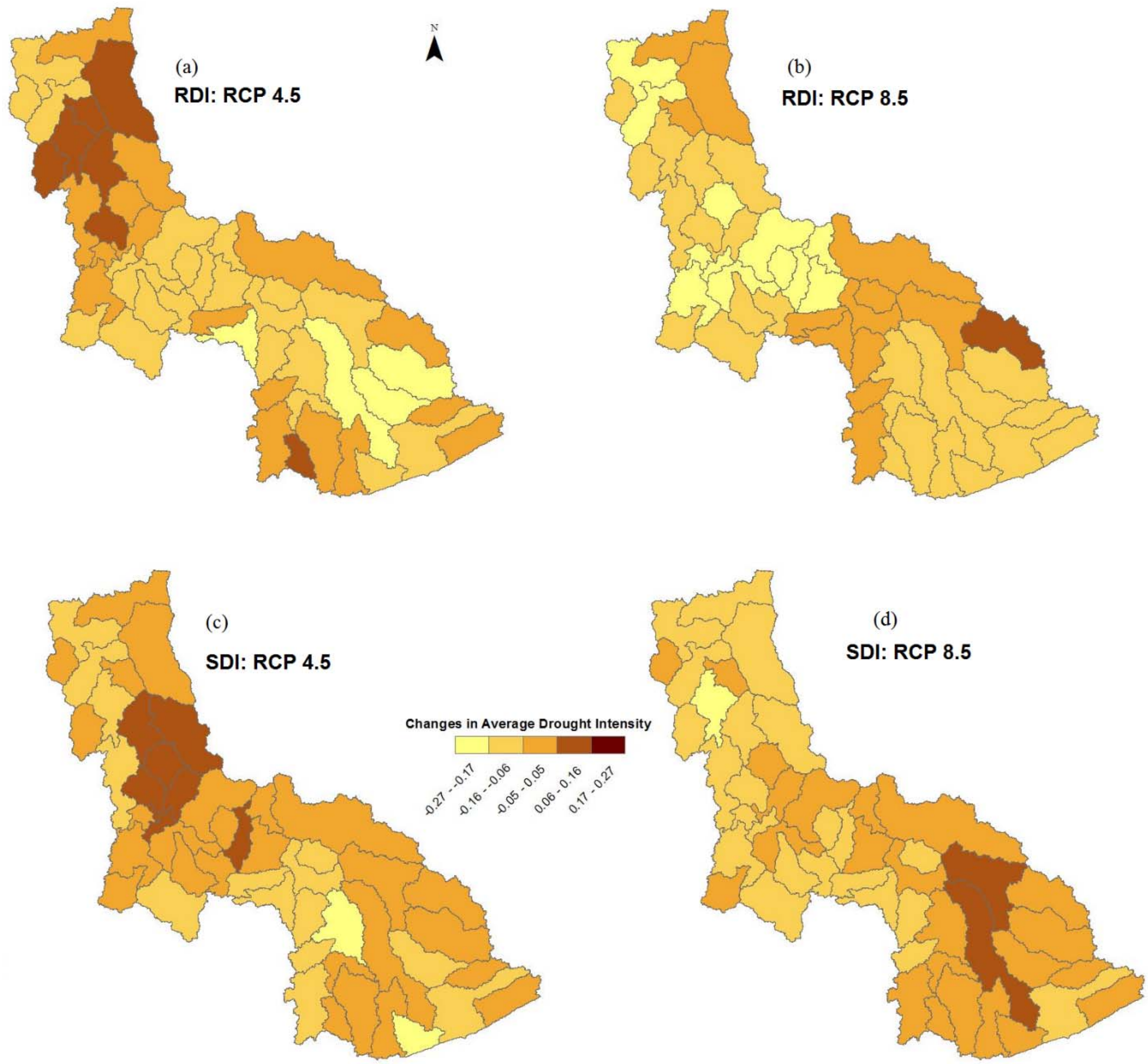

Figure 9. Spatial distribution of changes in drought intensity in the late-century calculated from RDI (a-b) and SDI (c-d) under RCP 4.5 and 8.5 respectively

References

Green, T. R., M. Taniguchi, H. Kooi, J. J. Gurdak, D. M. Allen, K. M. Hiscock, H. Treidel and A. Aureli, 2011. Beneath the surface of global change: Impacts of climate change on groundwater. Journal of Hydrology 405:532-560.

Haddeland, I., J. Heinke, H. Biemans, S. Eisner, M. Flörke, N. Hanasaki, M. Konzmann, F. Ludwig, Y. Masaki, J. Schewe, T. Stacke, Z. D. Tessler, Y. Wada and D. Wisser, 2014. Global water resources affected by human interventions and climate change. Proceedings of the National Academy of Sciences 111:3251-3256.

Diffenbaugh, N. S. and M. Ashfaq, 2010. Intensification of hot extremes in the United States. Geophysical Research Letters 37:n/a-n/a.

IPCC (Intergovernmental Panel on Climate Change). 2007. Climate change 2007: Impacts, adaptation and vulnerability. Contribution of working group II to the Fourth Assessment Report of the Intergovernmental Panel on Climate Change. Cambridge University Press.

Abatzoglou, J. T. and T. J. Brown, 2012. A comparison of statistical downscaling methods suited for wildfire applications. International Journal of Climatology 32:772-780.

Hong, X., S. Guo, Y. Zhou and L. Xiong, 2015. Uncertainties in assessing hydrological drought using streamflow drought index for the upper Yangtze River basin. Stochastic Environmental Research and Risk Assessment 29:1235-1247.

Tsakiris, G., D. Pangalou and H. Vangelis, 2007. Regional Drought Assessment Based on the Reconnaissance Drought Index (RDI). Water Resources Management 21:821-833

Information Transfer Program Introduction

Information transfer activities are an important part of the overall program of the Kentucky Water Resources Research Institute. There are two main components, an annual symposium and the institute web sites. The institute also participates and supports numerous other technology transfer activities throughout the year.

Kentucky information transfer project

Basic Information

Title:	Kentucky information transfer project
Project Number:	2016KY263B
Start Date:	3/1/2016
End Date:	2/28/2017
Funding Source:	104B
Congressional District:	KY 1-6
Research Category:	Not Applicable
Focus Category:	None, None, None
Descriptors:	None
Principal Investigators:	Lindell Ormsbee

Publication

1. Proceedings 2107 Kentucky Water Resources Symposium, Kentucky Water Resources Research Institute, Lexington, KY, 102 p.

Kentucky Information Transfer Project (2016KY263B)

Problems and Objectives

The Water Resources Research Act requires that Institutes or Centers shall:

1) plan, conduct, or otherwise arrange for competent applied and peer reviewed research that fosters -

(A) improvements in water supply reliability

(B) the exploration of new ideas that -

(i) address water problems; or

(ii) expand understanding of water and water-related phenomena;

(C) the entry of new research scientists, engineers, and technicians into water resources fields; and

(D) the dissemination of research results to water managers and the public.

2) cooperate closely with other colleges and universities in the State that have demonstrated capabilities for research, information dissemination, and graduate training in order to develop a statewide program designed to resolve State and regional water and water related land problems.

Each institute shall also cooperate closely with other institutes and other organizations in the region to increase the effectiveness of the institutes and for the purpose of promoting regional coordination.

Kentucky information transfer activities are conducted in support of these objectives.

Methodology

Information transfer activities are an important part of the overall program of the Kentucky Water Resources Research Institute. There are 2 main components, an annual symposium and the Institute's web sites. The Institute also participates in and supports other technology and information transfer activities throughout the year.

The Associate Director develops the program for the Annual Water Resources Symposium. Presentations in both platform and poster format allow researchers and practitioners to share progress on planned, ongoing, and completed water-related activities throughout the Commonwealth each year. Recipients of the 104(b) student research enhancement grants are required to present the results of their projects at the symposium.

The Information Specialist Senior assists with posting program announcements and the proceedings volume for the symposium on the web site. She develops and maintains content for several web sites including the main Institute page at: www.uky.edu/waterresources/. Links for additional sites describing projects and activities (for example, volunteer sampling results and watershed pages for the Kentucky River basin) are provided on the main web site. Research translation to make results accessible for a variety of audiences is a major goal for all of the technology transfer activities of the unit.

The Institute cooperates closely with other groups and agencies in planning additional technology transfer activities in the Commonwealth. These efforts included support for seminars/lectures, support for other web sites, and open houses during Earth Science Week and Engineering Day. Institute staff members serve a variety of support roles on technical committees and advisory panels for agencies and volunteer organizations to help disseminate relevant information about ongoing activities and research results.

Principal Accomplishments and Activities

Kentucky Water Awareness Month is an educational program of the University of Kentucky Cooperative Extension Service, Environmental and Natural Resources Issues (ENRI) Task Force (the Associate Director of KWRRI serves on this group). The program promotes overall water awareness for citizens of Kentucky During May each year. Materials are developed by a committee at the state level and distributed to all of the 120 county extension offices in the state. Individual county agents are encouraged to tailor the program to fit their county's specific needs and to use the materials to enhance their program efforts. The materials remain available throughout the year for use by classroom teachers, 4-H volunteers, and others interested in water issues through the ENRI internet site: www.ca.uky.edu/enri/ or directly at: http://water.ca.uky.edu/kwam. The Task Force is also working to encourage Project WET training for extension agents across the Commonwealth. A separate educational program for local elected officials is also under development to inform them of potential water resource issues in local communities.

Water Week, October 10-14, 2016, was a week-long series of events designed to inform faculty, staff, and students on the University of Kentucky campus of the importance of water in the environment. This was the second year of this annual fall event. The project was a collaborative between the College of Agriculture, Food, and the Environment, the College of Arts and Sciences, the College of Engineering, the Kentucky Geological Survey, the Tracy Farmer Institute for Sustainability and the Environment, and the Kentucky Water Resources Research Institute. Featured events for 2016 included: “Trash Talk: Tales from a Mississippi River Adventure” a presentation and discussion with Alyssum Pohl at lunch on Monday; “Big River” film screening, panel discussion, and dinner on Tuesday evening; Career Panel, networking opportunity, and dinner on Wedensday evening; a seminar “Sikhole Collapse” by Dr. Ming Ye of Florida State University on Thursday afternoon; and “CATchment Cleanup” a stormwater basin maintenance service learning opportunity led by the Biosystems and Agricultural Engineering student chapter on Friday afternoon. These events were organized by a multidisciplinary group of researchers working toward the advancement of water-related research and education at the University of Kentucky.

An open house was held on Wednesday evening 10/12/16 in association with Earth Science Week. This event was co-sponsored with the Kentucky Geological Survey. KWRRI staffed a water exhibit for the elementary, middle school, high school students, and their parents who attended the event (approximately 200 people).

Engineers Day, or E-Day, is a celebration of everything engineering has to offer at the University of Kentucky. From building bridges to discovering new medications to writing the software that powers our cell phones, engineers and computer scientists do the things that make the 21st-century world work. The 2017 E-Day celebration at the University of Kentucky in Lexington was on Saturday, Feb. 25, from 9 a.m. to 1 p.m. E-Day comes at the end of Engineers Week, an annual event sponsored by a coalition of more than 100 professional societies, major corporations and government agencies dedicated to promoting math and science literacy and ensuring a diverse and well-educated future engineering workforce. KWRRI staffed an Enviroscape exhibit demonstrating sources of nonpoint source pollution for participants at the event.

Cyberseminars provided through the Consortium for the Advancemnt of Hydrolgoic Sciences, Inc. were made available of the University of Kentucky Campus for interested faculty, staff, students, and local professionals. The initial University of Kentukcy membership in CUAHSI was underwritten by the KWRRI.

The Kentucky Water Resources Annual symposium was held on March 20, 2017. Although the date of the symposium fell outside of FY2016, most of the planning and preparation for the event occurred during the fiscal year. An opening plenary session featured 3 student presentations. This was followed by a session including 15 poster presentations. Two concurrent sessions provided time slots for 18 oral presentations. The noon luncheon provided an opportunity for presentation of annual awards acknowledging outstanding contributions in the areas of Water Research, Water Practice, and Water Quality. A second poster session in the afternoon provided an opportunity for 14 additional presentations. Approximately 120 people attended the meeting. Abstracts for all of the presentations were distributed to participants on the day of the meeting: Proceedings of the 2017 Kentucky Water Resources Annual Symposium, 2017, Kentucky Water Resources Research Institute, Lexington KY, 102 p. The full proceedings document is also available online through a link on the institute web site: www.uky.edu/waterresources/ The document includes contact information for all of the authors and presenters. Symposium participants also received a list of attendees providing basic contact information for each individual who pre-registered for the symposium. Attendees included researchers, personnel from local, state, and federal agencies, undergraduate and graduate students, participants from volunteer groups and NGOs, and members of the general public. Conference registration fees are kept low through partial subsidy of symposium expenses (using 104(b) technology transfer and matching funds) to ensure accessibility to individuals from all potential audiences. All of the 104(b) student research enhancement projects funded through the Institute during FY2016 presented their results at the symposium.

Maintenance of the institute web site provides open access for those interested in the activities of the Institute. The site also provides additional links to related sites and information maintained by others. Creation and maintenance of the web site are ongoing throughout the year. Links on the site provide direct access to the Kentucky Center of Excellence for Watershed Management, the University of Kentucky Superfund Research Center, the Kentucky Research Consortium for Energy and Environment, the Kentucky River Watershed Watch, the Tracy Farmer Institute for Sustainability and the Environment, the Environmental Research and Training Laboratory, and the Kentucky Geological Survey.

Over the past two or three years, the KWRRI has worked with colleagues across Southeastern Athletic Conference institutions to propose a water-themed symposium. The primary goal of this academic conference-type event was to address a significant scholarly issue utilizing the range of disciplinary strengths of all SEC universities in a manner that expands opportunities for collaboration among SEC faculty and administrators and draws national attention and participation to the Southeast region. This event is also intended to display the research and innovation of SEC institutions for an audience of academicians, government officials and other stakeholders. The university presidents and provosts ultimately accepted a proposal for a water-themed conference. Planning for the regional event ultimately held in Starkville Mississippi on March 27-28, 2017 took place throughout the FY2016 funding cycle. A separate track was set aside for NIWR institute planning and networking during the conference.

USGS Summer Intern Program

None.

Student Support					
Category	**Section 104 Base Grant**	**Section 104 NCGP Award**	**NIWR-USGS Internship**	**Supplemental Awards**	**Total**
Undergraduate	5	0	0	0	5
Masters	4	0	0	0	4
Ph.D.	4	0	0	0	4
Post-Doc.	0	0	0	0	0
Total	13	0	0	0	13

Notable Awards and Achievements

2016KY260B - Hannah Conley received a merit award from Morehead State University for her poster presentation: Conley, H., R. Brown, G.W. Gearner, The use of eDNA to detect bacterial molecular markers in the Triplett Creek Watershed, presented at the Celebration of Student Scholarship, Morehead State University, Morehead, KY, April 26, 2017.

2016KY257B - Jake Hutton, an MS student under Dr. Price is building upon the research effort originally established in this project. He has received several awards to support follow up on this work: Casner Fellowship Program, University of Kentucky ($1500); Eastern Kentucky University Division of Natural Areas Grant-in-Aid ($800), Society of Freshwater Science Conservation Research Award ($1000); and a grant from the Foundation for the Conservation of Salamanders ($5000).